A new Kalman filter approach for structural parameter tracking: application to the monitoring of damaging structures tested on shaking-tables

M. Diaz[a,b,*], P.-É. Charbonnel[b], L. Chamoin[a,c]

[a] *Université Paris-Saclay, CentraleSupelec, ENS Paris-Saclay, CNRS, LMPS - Laboratoire de Mécanique Paris-Saclay, 91190, Gif-sur-Yvette, France*

[b] *DES-Service d'Études Mécaniques et Thermiques (SEMT), CEA, Université Paris-Saclay, 91191 Gif-sur-Yvette, France*

[c] *IUF, Institut Universitaire de France*

Abstract

In this paper, a new data assimilation framework for correcting finite element models from datasets acquired on-the-fly in low-frequency dynamics is presented. An Unscented Kalman filter algorithm is coupled with a modified Constitutive Relation Error (mCRE) observer, leading to a Modified Dual Kalman Filter algorithm (MDKF). Built as a Hermitian data-to-model distance written in the frequency domain enriched with a CRE residual accounting for model bias, the mCRE functional has shown interesting assets for model updating purposes, in particular enhanced convexity and robustness to measurement noise. The proposed data assimilation strategy integrates the latter through a metric change in the measurement update equation. It thus differs from classical nonlinear Kalman filtering for parameter estimation as the comparison between measurements and model predictions is achieved through the mCRE functional itself. Besides, the calibration of MDKF internal parameters is facilitated by a set of general guidelines that ensure the performance of the algorithm. The methodology is applied to two earthquake engineering examples. The performances of MDKF are first assessed using synthetic measurements from a plane frame subjected to random ground acceleration. Actual measurements from the SMART2013 benchmark are then assimilated in a real-time context to monitor the eigenfrequency drop of a reinforced-concrete structure submitted to a sequence of gradually damaging shaking-table tests. The nice correlation with (i) data-driven identification results, and (ii) sequential mCRE-based model updating results, illustrates the relevance of this new approach and suggests promising use of MDKF for on-the-fly adaptive control prospects and applications involving data-to-model interaction.

Keywords: Kalman Filter, Modified Constitutive Relation Error, Low-Frequency Dynamics, Online model updating, Earthquake Engineering

*Corresponding author
Email address: matthieu.diaz@ens-paris-saclay.fr (M. Diaz)

1. Introduction

The design, analysis and prediction of dynamical systems requires the construction of robust numerical models. These models can be directly built from measurements (*black-box modeling*) or derived after in-depth physical description of the involved phenomena (*white-box modeling*). In each case, as most of modern systems are now equipped with numerous sensors, those models are assessed by comparison with experimental data in order to define their degree of validity. The dialogue between physics-based models and experimental data has become of major importance in the last two decades with the emergence of new paradigms such as *Digital Twins* [1–3], that combine physics-based (usually reduced-order) models and data-science. Moreover, in *Dynamic Data-Driven Application Systems* (DDDAS) [4, 5], a close (online) dialogue is established between numerical models and experimental data with a dual objective: (i) controlling the evolution of the experimental system thanks to model predictions and (ii) updating the numerical model by feeding it with some measurements acquired in real-time.

Earthquake engineering problems are no exception to the need of using experimental data to build, validate and operate robust numerical models. For instance, the integration of experimental data in model-based approaches provides new techniques for monitoring the occurrence, formation and propagation of structural damage when assessing the safety of structures in Structural Health Monitoring (SHM) [6] and vibration-based structural damage detection [7]. Another way to assess the response of structures under dynamic loading is to characterize them directly in laboratory conditions. In this context, the CEA/TAMARIS facility carries out seismic tests using shaking-tables moved by high-power hydraulic actuators on complete or partial structures at real or reduced scale. Controlling the hydraulic actuators of the shaking-tables is still a challenging task that emphasizes the need of establishing a close dialogue between model and measurements (see Fig. 1). Indeed, the modal signature of damaging specimens can suddenly change under seismic loading conditions [8]. As modal signature is the key input-feature for linear control law design, the initial control strategy may become inappropriate, leading to unstable experiments. The lack of representativeness of numerical models to predict such phenomena therefore imposes to carry out test sequences of increasing level where control laws are iteratively corrected from one test to another to account for the observed eigenfrequency drops and dynamic impedance changes [9].

The ambition of this work is to contribute to the integration of Finite Element (FE) models in the shaking-tables control strategy by resorting to a close and dynamic data-to-model interaction (see Fig. 1). From a numerical viewpoint, the application of DDDAS requires data assimilation (sequential solution of inverse problems) and optimal control, which are, in general, computationally demanding tasks, especially when complex models derived from partial differential equations are used. In this paper, we focus on the identification/update loop of Fig. 1 and we propose to this end a new Kalman filter-based approach for real-time data assimilation where the offline model updating framework developed in [10] is reinvested in order to perform robust on-the-fly structural parameter tracking.

First considering the model updating problem itself, it is well-known that identifying a set of internal model parameters requires the solution of an underlying inverse problem,

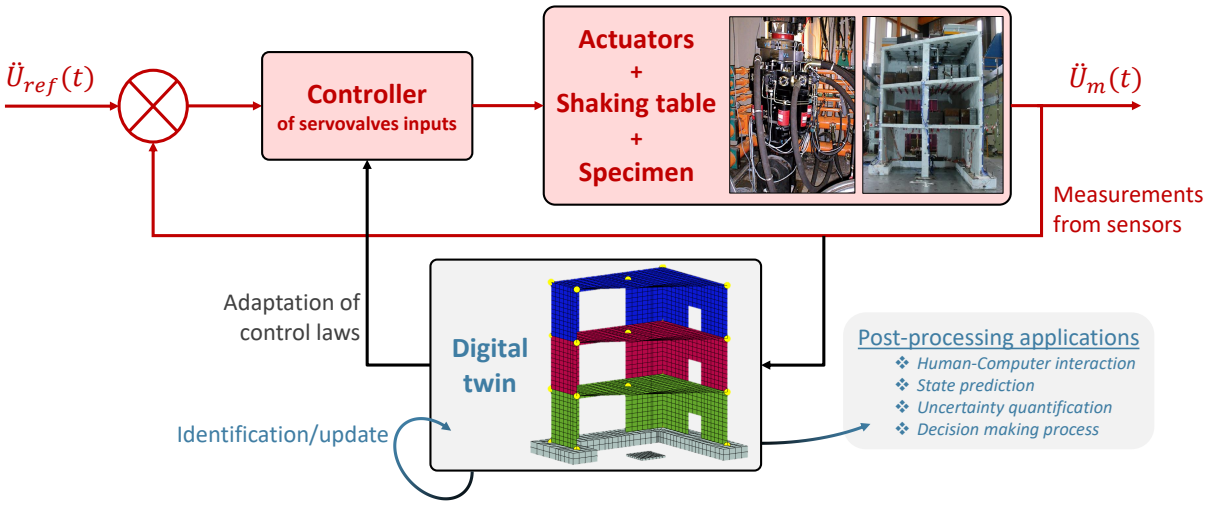


FIGURE 1: DDDAS framework for the control of shaking-tables - introduction of a numerical model updated on-the-fly for optimal control law design.

which is often ill-posed in the Hadamard sense [11, 12]. Classically, to solve such problems, deterministic approaches [11, 13–15] based on the definition and the minimization of a data-to-model distance may be considered. Alternatively, stochastic methods leaning on the Bayesian inference framework may be used in order to represent uncertainties on parameters described by probability density functions (pdfs) [12, 16, 17].

Low-Signal-to-Noise Ratio (low-SNR) measurements from typical seismic inputs may be harder to integrate as experimental data to update FE models properly. An alternative to the above-mentioned classical techniques then consists in using the concept of *modified Constitutive Relation Error* (mCRE). Initially proposed for model updating in dynamics [18–22] by Ladevèze and co-workers, the mCRE functional is defined as a quadratic model-to-measurements distance enriched with a term based on the concept of *Constitutive Relation Error* (CRE) [23]. The idea behind this enrichment is to improve the ellipticity properties of the cost function by adding a term which has a strong mechanical content and relaxes the most unreliable parts of the model description. This energy-based residual offers interesting advantages. First, it improves local convexity properties compared to classical least-square functionals [24]. Besides, the CRE part of the residual, computed over the whole structure, allows to select the most erroneous areas in order to restrain the updating process to a few parameters [25]; this provides valuable regularization (in the Tikhonov sense), particularly when the number of parameters to update becomes important. The numerous applications of mCRE for model updating during the last two decades have proven its robustness in a wide range of applications. Among them, it is worth mentioning robustness to highly noisy or even corrupted measurements [26, 27], local defect detection [28, 29], full-field material identification [30–32], or coupling with model order reduction for real-time prospects [33]. Recently, the mCRE-based model updating algorithm has been fully automated in low-frequency dynamics, with enhanced robustness with respect to measurement noise and a dedicated formulation to improve performance when dealing with random inputs [10]. In

particular, promising offline model updating results have been obtained when processing acceleration recordings from actual shaking-table tests. These developments will be reinvested in this contribution.

To adapt the previous model updating framework to the online correction of FE models, data assimilation techniques must be involved. Among them, Kalman Filtering (KF) is probably one of the most common and popular algorithms. Introduced in the 1960s, the Kalman filter is a sequential stochastic data assimilation method derived from the Bayes theorem, that initially applies to linear dynamical systems under Gaussian assumptions [34, 35]. The algorithm is made of a recursive prediction-correction scheme, where model predictions are incrementally corrected based on assimilated measurements. Several extensions of KF to handle nonlinear models have been proposed in the last decades. One can classically divide them in two families:

- Methods based on operator linearization; the *Extended Kalman Filter* (EKF) is based on this principle and is probably one of the most popular approaches in the literature, both for state and parameter estimation [36];
- Methods based on statistical regularization; these techniques are based on the fact that sampling points transformed by nonlinear operators enable to approximate state statistics correctly. We particularly refer here to the *Ensemble Kalman Filter* (EnKF) [37] or *Particle Filters* (PF) [38] where a Monte-Carlo sampling is propagated through the nonlinear operators at each data assimilation step, and to the *Unscented Kalman Filter* (UKF) whose sampling points set is of reduced size by means of a deterministic selection (the eponymous *Unscented Transform*) [39–42].

In addition, parameter estimation techniques using the *Dual* or *Joint* extensions of nonlinear KFs have also been developed. Although EKF was used first for model updating purposes in structural dynamics [43], UKF was also largely used for similar applications. Among dedicated studies involving UKF for the characterization of nonlinear phenomena in dynamics, it is worth mentioning the works of Azam and co-workers [44–48] for online damage detection and state prediction in structural (nonlinear) dynamics. A dedicated comparison between EKF and UKF in nonlinear structural dynamics was proposed in [49], and real-time data assimilation prospects have also been investigated in [50]. Several modifications of UKF, especially to save CPU time by introducing reduced order modelling techniques, were also discussed in [51, 52]. More recent works intended to apply UKF (and EKF) to update classical nonlinear reinforced concrete models based on earthquake engineering experiments [53–55]. In parallel, the performance of the different KF algorithms has been extensively compared [53, 56–59], highlighting that UKF is often more efficient than EnKF in terms of CPU time, and outperforms EKF for an equivalent computational cost: this is the main driver behind its selection as a reference method for sequential data assimilation in this paper.

In this contribution, a new Kalman filter-based data assimilation strategy inspired from the developments of [60] in quasi-statics is proposed for on-the-fly model updating in low-frequency dynamics. The offline mCRE-based model updating algorithm [10] is extended to an online data assimilation strategy by coupling it with a nonlinear dual UKF, leading to the so-called *Modified Dual Kalman Filter* algorithm (MDKF).

The key idea of the proposed methodology is to introduce the mCRE as a new observation operator in a dual UKF context. This change in the metric of the KF measurement update equation allows MDKF to provide parameter estimates that are sought as minimizers of the mCRE functional. It thus avoids direct confrontation between experimental data and model predictions. In low-frequency dynamics, the fact that the mCRE operates in the frequency domain implies that a dedicated effort must be made to define how measurements are integrated into the mCRE functional. This problem does not appear with classical KFs as observation operators are most of the time linear projection matrices. In the MDKF algorithm, a sliding window technique is proposed to progressively add new data points before processing measurements in the frequency domain. The progressive assimilation of data and the inherent properties of mCRE provide an enhanced robustness to measurement noise compared to classical KFs for parameter estimation. Although this new framework seems more complex to operate, general guidelines based on physical meaning and engineering judgement are provided regarding the calibration of internal parameters (KF error covariance matrices in particular). A dedicated sensitivity analysis on these internal parameters is also proposed in the following, showing that even suboptimal choices for internal parameters can lead to relevant assimilation results. Finally, dedicated strategies are proposed to ensure low computational times. The efficiency of the MDKF is illustrated using both synthetic measurements and actual test results from the SMART2013 benchmark. The successful use of MDKF in both cases emphasizes the relevance of this new methodology for online model updating from sparse and noisy data. As shown using synthetic measurements, MDKF is able to track evolutive structural parameters, allowing to perform structural monitoring by interpreting the estimated stiffness loss as overall damage (as long as sufficiently rich and dense measurements are available). Although the limited amount of data in the SMART2013 case does not allow us to localize damaged areas accurately, the MDKF can still be used as an alternative to classical modal identification techniques to perform model-based modal tracking. The possibility to provide relevant estimates of eigenfrequencies in real-time during damaging tests is a valuable asset for control law design prospects. It thus presents MDKF as an appropriate tool for model-based control applications in the DDDAS framework of Fig. 1.

The paper is structured as follows: Section 2 recalls basics on Kalman filtering and mCRE for low-frequency dynamics, which are the two main ingredients of the methodology introduced in this work. Section 3 gives more insights into the MDKF algorithm, from its general formulation to technical details; the complete algorithm is also explicitly given. Section 4 presents the results of the two numerical applications processed in this work. An earthquake-engineering-inspired academic example (plane frame submitted to random ground acceleration loading) enables a full discussion on the efficiency of the methodology with respect to measurement noise of known level and comparison with classical KF-based approaches. The results obtained processing the SMART2013 database are then detailed: after a short contextualization and description of the FE model borrowed from [9], results obtained when processing (in real-time) the whole database with MDKF are finally presented and discussed. The good correlation between (*i*) the updated modal signature obtained after using the novel MDKF algorithm, (*ii*) the identified modal signature using an automated mCRE-based model updating algorithm from [10], and (*iii*) the modal identification results

formerly obtained using data-driven subspace-based algorithms [8], illustrates the relevance of the proposed data assimilation methodology. Conclusions and prospects are finally drawn in Section 5, suggesting promising future use of MDKF for the design of model-based control laws in shaking-table experiments.

2. Basics on Kalman filtering and modified Constitutive Relation Error

2.1. Unscented Kalman filter for parameter estimation

2.1.1. UKF at a glance

The starting point of the KF theory is the definition of a dynamical system under state-space discrete form (1). This system is made of two equations:

$$\begin{cases} x_{k+1} &= \mathcal{M}(x_k, \theta, u_k) + w_{x,k} \\ y_k &= \mathcal{H}(x_k, u_k) + v_k \end{cases} \tag{1}$$

where $x_k \in \mathbb{R}^{n_x}$ is the state vector at time point t_k, $y_k \in \mathbb{R}^{n_y}$ is the vector of observations, while the two (uncorrelated) zero-mean Gaussian white-noise terms $w_{x,k} \in \mathbb{R}^{n_x} \sim \mathcal{N}(0, Q_x)$ and $v \in \mathbb{R}^{n_y} \sim \mathcal{N}(0, R)$ respectively shape model uncertainties and measurement noise. Matrices Q_x and R are the so-called model and measurement covariance error matrices. They are here assumed diagonal, constant with time and defined as: $Q_x = \mathbf{E}\left(w_{x,k} w_{x,k}^T\right)$; $R = \mathbf{E}\left(v_k v_k^T\right)$ where $\mathbf{E}(\square)$ refers to the mathematical expectation operator. The dynamical system (1) is based on two (possibly nonlinear) operators, namely the model operator $\mathcal{M}$ and the observation operator $\mathcal{H}$. The latter classically extracts partial information regarding the predicted state x_k or inputs u_k. Finally, note that model predictions also depend on a set of internal parameters $\theta \in \mathbb{R}^{n_\theta}$ (*e.g.* material properties).

The *Unscented Kalman Filter* (UKF) is a nonlinear version of the KF algorithm that keeps a very similar algorithmic structure. The state x_k is also modelled as a set of Gaussian Random Variables (GRVs) whose mean and covariance error matrix are estimated by a prediction/correction scheme:

(i) In the prediction step, the state update equation is exploited to provide *a priori* mean $\widehat{x}_{k+1|k}$ and covariance error matrix $P^x_{k+1|k}$ according to last estimates $\widehat{x}_k$ and P^x_k. Observations are also predicted to be compared with actual measurements;

(ii) In the correction step, predictions are corrected based on the new measurements y_k, leading to the updated mean $\widehat{x}_{k+1}$ and covariance error matrix P^x_{k+1}.

The specificity of UKF is that it exploits the eponymous *Unscented Transform* (UT) which allows to represent mean and covariance of GRVs accurately up to the third order (whatever the involved nonlinearities) using a set of deterministic well-chosen samples, called sigma-points $\mathcal{X}_k$. UKF prediction and correction steps thus mainly consist in propagating the set of sigma-points through the nonlinear model and observation operators, the statistics of x_k being computed by weighted sum (the sigma-points weights $(\mathcal{W}^m, \mathcal{W}^c)$ being also given by the UT). The overall recursive UKF algorithm is presented in Alg. 1.

Please note that for the sake of conciseness, this section only overviews UKF fundamental equations but does not go into much details regarding the UT itself. The interested reader is referred to [39–41] for complementary explanations.

2.1.2. Extension to parameter identification

The previous KF framework allows to update the state vector in data assimilation processes. Much research works in the last decades have been dedicated to its extension for the identification of uncertain model parameters.

These parameters must be explicitly integrated to the dynamical system (1) in order to identify them in a KF framework. Without any *a priori* knowledge, one can formulate a simple stationary evolution law, although it remains a restrictive hypothesis (*e.g.* damage is not). The stationarity assumption is thus relaxed with the addition of a zero-mean Gaussian white-noise $w_{\theta,k} \in \mathbb{R}^{n_\theta} \sim \mathcal{N}(0, Q_\theta)$ so as to shape uncertainty on parameters and permit their evolution during the data assimilation process. The covariance error matrix on parameters is also assumed constant with time in this work and thus defined as $Q_\theta = \mathbf{E}\left(w_{\theta,k} w_{\theta,k}^T\right)$. Therefore, the full dynamical system (1) now reads:

$$\begin{cases} \theta_{k+1} &= \theta_k + w_{\theta,k} \\ x_{k+1} &= \mathcal{M}_k(x_k, \theta_k, u_k) + w_{x,k} \\ y_k &= \mathcal{H}_k(x_k, u_k) + v_k \end{cases} \tag{2}$$

In the above-mentioned works [43–55], two formulations are used to apply nonlinear KF to the system (2): *Joint* and *Dual* Kalman filters. Concisely, the joint Kalman filter consists in a direct concatenation of state and parameters vectors into a joint state $x_k^\star = [x_k^T \ \theta_k^T]^T$, leading to a joint model operator:

$$\begin{cases} x_{k+1}^\star &= \begin{bmatrix} \mathcal{M}(x_k, \theta_k, u_k) + w_{x,k} \\ \theta_k + w_{\theta,k} \end{bmatrix} \\ y_k &= \mathcal{H}(x_k^\star, u_k) + v_k \end{cases} \tag{3}$$

On the contrary, the dual Kalman filter chooses the set of internal parameters as state vector. This implies to turn the observer (often a projector when considering classical KFs) into a state evaluation operator $\mathcal{H}_{dual}$:

$$\begin{cases} \theta_{k+1} &= \theta_k + w_{\theta,k} \\ y_k &= \mathcal{H}_{dual}(x_k, \theta_k, u_k, w_{x,k}) + v_k \end{cases} \tag{4}$$

This new observer is itself based on a second Kalman filter (which is at the origin of the *dual* denomination) that allows to provide statistics on the state vector x_k for a given set of internal parameters. Both methods have been equally implemented in former works and even compared (see [57] for a complete study in structural dynamics). Even though dual KF may provide slightly better estimates, the combined use of two KF also introduces more user-defined parameters (especially process and observation noise covariance matrices Q_x, Q_θ, R), whose calibration is not an easy task [61].

Algorithm 1: Unscented Kalman Filter.

Initialization:

- Model and observation operators: $\mathcal{M}, \mathcal{H}$
- Internal model parameters θ and loading conditions: $u_{0:\infty}$
- Noise process and measurements covariance matrices: Q_x, R
- Initial state vector $\widehat{x}_0 = \mathbb{E}[x_0]$ and associated covariance matrix P_0^x
- Sigma-points weights $\{\mathcal{W}_i^m, \mathcal{W}_i^c\}_{i=0}^{2L}$ with $L = \dim(\widehat{x}_0)$

for $k = 0 : \infty$ **do**

1) **Unscented Transform**

Augmented state to include noise parameters:
$\widehat{x}_k^a = \left[\widehat{x}_k^T \; w_{x,k}^T \; v_k^T\right]^T$; $P_k^{x,a} = \text{diag}(P_k^x, Q, R)$;
Computation of sigma-points:
$\mathcal{X}_k^a = \left[\widehat{x}_k^a \quad \dots \; \widehat{x}_k^a + \sqrt{L+\lambda}\left[P_k^{x,a}\right]_j^{1/2} \; \dots \quad \dots \; \widehat{x}_k^a - \sqrt{L+\lambda}\left[P_k^{x,a}\right]_j^{1/2} \; \dots\right]$
with $j = 1, ..., 2L$, λ a UT parameter and $\left[P_k^{x,a}\right]_j^{1/2}$ the jth column of the of the Cholesky decomposition of $P_k^{x,a}$;

2) **Prediction step**

Propagation of the sigma-points through the state update equation:
$\mathcal{X}_{k+1|k}^i = \mathcal{M}(\mathcal{X}_k^{i,x}, \theta, u_k) + \mathcal{X}_k^{i,w} \; \forall i \in [\![0; 2L]\!]$;
Computation of *a priori* mean and covariance:

$$\widehat{x}_{k+1|k} = \sum_{i=0}^{2L} \mathcal{W}_i^m \mathcal{X}_{k+1|k}^{i,x} \; ;$$

$$P_{k+1|k}^x = \sum_{i=0}^{2L} \mathcal{W}_i^c \left(\mathcal{X}_{k+1|k}^{i,x} - \widehat{x}_{k+1|k}\right)\left(\mathcal{X}_{k+1|k}^{i,x} - \widehat{x}_{k+1|k}\right)^T \; ;$$

3) **Correction step**

Propagation of the sigma-points through the observation equation:
$\mathcal{Y}_{k+1|k}^i = \mathcal{H}(\mathcal{X}_{k+1|k}^{i,x}, u_k) + \mathcal{X}_k^{i,v} \; \forall i \in [\![0; 2L]\!]$;

$$\widehat{y}_{k+1|k} = \sum_{i=0}^{2L} \mathcal{W}_i^m \mathcal{Y}_{k+1|k}^i \; ;$$

$$P_{k+1|k}^{yy} = \sum_{i=0}^{2L} \mathcal{W}_i^c \left(\mathcal{Y}_{k+1|k}^i - \widehat{y}_{k+1|k}\right)\left(\mathcal{Y}_{k+1|k}^i - \widehat{y}_{k+1|k}\right)^T \; ;$$

$$P_{k+1|k}^{xy} = \sum_{i=0}^{2L} \mathcal{W}_i^c \left(\mathcal{X}_{k+1|k}^{i,x} - \widehat{x}_{k+1|k}\right)\left(\mathcal{Y}_{k+1|k}^i - \widehat{y}_{k+1|k}\right)^T \; ;$$

Correct predictions with new measurements to compute *a posteriori* statistics:
$\widehat{x}_{k+1} = \widehat{x}_{k+1|k} + K_k(y_{k+1} - \widehat{y}_{k+1|k})$
$P_{k+1}^x = P_{k+1|k}^x - K_k P_{k+1|k}^{yy} K_k^T$
with $K_k = P_{k+1|k}^{xy}(P_{k+1|k}^{yy})^{-1}$ the Kalman gain matrix

end

Result: Recursive estimates of the state vector mean and covariance error matrix

2.2. The mCRE for model updating in low-frequency dynamics

This section intends to briefly recall the fundamentals of the mCRE-based model updating framework for low-frequency dynamics, starting from a linear FE problem written in the frequency domain. Particular attention is paid to the construction of the *Constitutive Relation Error* (CRE) residual from the set of equations defining the reference mechanical problem. Then, details about the *modified Constitutive Relation Error* (mCRE), which is the extension of CRE for model updating problems, are explicitly given considering the correction of stiffness parameters. The interested reader is referred to [10, 21, 25] for comprehensive overviews of the offline mCRE-based model updating framework for low-frequency dynamics.

2.2.1. The CRE as modelling error

Let us consider a linear elastic structure submitted to dynamic loading conditions. The reference problem discretized in a FE framework leads to the general dynamic equilibrium equation, that is written in the frequency domain at a given angular frequency ω as:

$$\left[-\omega^2 M + i\omega D + K\right] U_\omega = F_\omega \tag{5}$$

K, D, M denote the stiffness, damping and mass FE matrices, respectively, while F_ω and U_ω are the frequency counterparts of nodal loading conditions and displacement field. The key idea for the construction of the CRE residual lies into the distinction between reliable and unreliable information on the reference mechanical problem. Although this separation is non-unique and deeply relies on the case study and engineering expertise, the common case is given in Tab. 1 as constitutive relations are most of the time considered less reliable.

	Reliable	**Unreliable**
Model	• Geometry • Kinematic boundary conditions • Equilibrium equations	• Constitutive relations
Experimental data	• Loading frequencies ω • Sensors position and orientation • Measured inputs F_ω	• Measured outputs Y_ω

Table 1: Classical distinction between reliable and unreliable information for model updating in dynamics.

In this contribution, following the work of [10], the elastic part of the constitutive relations will be subject to caution. However, the dissipative part of the latter will not, as its impact on frequency response functions and shaking table control laws is secondary.

Indeed, considering shaking table control laws, the damage-induced increase of damping observed in RC specimens (friction at RC cracks lips level and rebars/concrete matrix sliding phenomena) naturally increases the stability of the specimen, which does not lead to control instabilities, contrary to abrupt eigenfrequency drops that can lead to unstable poles of the controlled system. Besides, it is a current practice when correcting frequency response functions in low-frequency dynamics to update stiffness properties in a first stage, before

updating damping properties in a second stage to update the sharpness of the resonant peaks once eigenfrequencies have been correctly calibrated.

Therefore, it is chosen in the following to consider only stiffness properties as unreliable. Note that considering the update of damping properties would lead to the mCRE framework described in [19, 21, 25] where the concept of dissipation error residual is introduced.

Doing so, the parameters to update θ only affect the stiffness matrix K and two admissibility spaces are implicitly defined:

(i) a kinematic admissibility space $\mathcal{U}_{ad}$ inside which any displacement field U verifies the reliable kinematic equations of the problem,

(ii) an auxiliary dynamically admissibility space $\mathcal{D}_{ad}$ defined as the set of displacement fields V derived from the stress field verifying the dynamic equilibrium. In other words, V represents the model-predicted response caused by unbalanced elastic forces.

Therefore, doubt is put on the constitutive relations. The reciprocity gap between $\mathcal{U}_{ad}$ and $\mathcal{D}_{ad}$ can be measured using an energy norm - the CRE - that estimates the relevance a solution couple $s_\omega = (U_\omega, V_\omega) \in \mathcal{U}_{ad} \times \mathcal{D}_{ad}$ with respect to the mechanical problem. With the above notations, the CRE at a given angular frequency ω reads:

$$\zeta_\omega^2(s_\omega, \theta) = \frac{1}{2}(U_\omega - V_\omega)^H K(\theta)(U_\omega - V_\omega) = \frac{1}{2}\left\|U_\omega - V_\omega\right\|^2_{K(\theta)} \tag{6}$$

The CRE provides a direct insight regarding the validity of the model itself, making it a relevant tool for identifying erroneous parts of the model as all finite element contributions to CRE can be computed independently.

2.2.2. Model updating problem including both CRE and measurements

The extension of the CRE concept to unreliable experimental data (see Tab. 1) directly leads to the so-called *modified Constitutive Relation Error* (mCRE). This energy-based residual is composed of two terms: the CRE itself ζ_ω^2 measuring the degree of non-verification of the elastic part of the constitutive relations, and a model-to-data distance from the predictions U_ω to the frequency counterpart of measurements Y_ω :

$$e_\omega^2(s_\omega, \theta, Y_\omega) \triangleq \zeta_\omega^2(s_\omega, \theta) + \frac{1}{2}\frac{r}{1-r}\left\|\Pi U_\omega - Y_\omega\right\|^2_{G_y} \tag{7}$$

The projection operator Π enables to extract predicted measured components of U_ω at corresponding sensors positions and directions. The choice of the symmetric positive-definite matrix G_y is not critical, however special care should be taken for guaranteeing that $\|\square\|_{G_y}$ is homogeneous to ζ_ω^2 and equivalent in level. A classical choice for G_y is to use the Guyan reduction of the initial stiffness operator condensed on the sensors locations [10, 21, 25]. The tuning factor $r \in]0;1[$ enables one to give more or less confidence to the measurements; close-to-unit values can be specified when measurements are considered reliable whereas close-to-zero values are better suited to corrupted or noisy recordings. The choice of r is therefore crucial for providing relevant parameter estimates. A procedure based on the a

priori optimal balance between measurement error and CRE has been proposed in recent works [10, 32] for its automated calibration.

The model updating procedure is conducted on a given frequency bandwidth D_ω which contains the essential information about the response of the structure. The complete mCRE functional $\mathcal{J}$ to be minimized is thus obtained by direct integration over D_ω:

$$\mathcal{J}(\theta, Y) = \int_{D_\omega} z(\omega) e_\omega^2(\widehat{s}(\theta, Y_\omega), \theta, Y_\omega) \, \mathrm{d}\omega \tag{8}$$

where $z(\omega)$ is a frequency weighting function such that $\int_{D_\omega} z(\omega) \, \mathrm{d}\omega = 1$ allowing to modulate the importance of specific frequencies of D_ω. Indeed, a frequency weighting function derived from the experimental frequency content enables to automatically favor the vicinity of the experimental eigenfrequencies; this enhances the robustness of the functional to measurement noise in low-frequency dynamics [10].

We denote by $\widehat{s}(\theta, Y_\omega)$ the optimal solution in the mCRE sense for given parameters and measurements, which is defined as

$$\forall\ \omega, \quad \widehat{s}(\theta, Y_\omega) \ = \ \arg \min_{[-\omega^2 M + i\omega D] U_\omega + K(\theta) V_\omega = F_\omega} e_\omega^2(s, \theta, Y_\omega) \tag{9}$$

Introducing Lagrange multipliers $\widehat{\Lambda}_\omega$ and an augmented cost function, it is easy to show that this constrained minimization problem is equivalent to the solution of the following linear system:

$$A \left\{ \begin{array}{c} \widehat{\Lambda}_\omega \\ \widehat{U}_\omega \end{array} \right\} = b \text{ with } \left\{ \begin{array}{rcl} \widehat{\Lambda}_\omega & = & \widehat{U}_\omega - \widehat{V}_\omega \\ A & = & \left[\begin{array}{cc} \left[K(\theta) + i\omega D - \omega^2 M\right]^H & \frac{r}{1-r} \Pi^H G_y \Pi \\ -K^H(\theta) & \left[K(\theta) + i\omega D - \omega^2 M\right] \end{array} \right] \\ b & = & \left\{ \begin{array}{c} \frac{r}{1-r} \Pi^H G_y \, Y_\omega \\ F_\omega \end{array} \right\} \end{array} \right. \tag{10}$$

whose size can be drastically reduced using projection on a reduced basis (*e.g.* truncated modal basis enriched with Krylov vectors) [21].

3. The Modified Dual Kalman Filter (MDKF)

As previously mentioned in Section 2.1, nonlinear KFs are relevant tools for updating on-the-fly the numerical models of dynamical (and evolutive) systems. They permit to track and identify accurately structural parameters from sparse and noisy measurements. Although recent works have presented adaptive techniques for automating their choice [54, 55, 61], the calibration of the covariance error matrices still remains a difficult task as the miscalibration of matrices Q_x, Q_θ, R may lead to irrelevant results. The lack of robustness of KFs with respect to measurement noise can limit their performance as well. In this contribution, with the aim of overcoming these inherent limitations, a new algorithm for sequential data assimilation in low-frequency dynamics is proposed - the Modified Dual Kalman Filter - whose formulation and algorithmic details are discussed in the remainder of this section.

3.1. MDKF formulation: change of metrics in the observation equation

Although the common definition of a projection matrix as observer seems rather intuitive since sensors directly collect measurements to be compared to model predictions, the choice of the observation metric (and thus the way measurements are processed) can be reconsidered for enhanced robustness with respect to measurement noise. In that sense, the developments initiated in [60] differ from the classical nonlinear KF framework for parameter estimation as the metric space of the observer is no longer the typical L^2-norm guaranteeing the convergence of state estimates towards measurements.

From the dual KF, one can choose to replace the dual observation operator (classically being a state prediction Kalman filter) with another functional able to quantify the closeness between model predictions and assimilated measurements. In this contribution, relying on advances that have been performed in the tailoring of mCRE to low-frequency dynamics [10], the proposed modified Dual Kalman Filter (MDKF) derives the mCRE as new observer operator in a dual Kalman filter framework. Practically, in a similar manner as one would compute optimal parameters minimizing the functional $\mathcal{J}$ from (8), the observation equation of the MDKF will reinvest the mCRE gradient $\nabla\mathcal{J}$ in order to guarantee the stationarity of the cost function. Please note that no additional numerical error is made with the call to the mCRE gradient as its analytical expression can be explicitly derived from the constrained minimization problem (10) (see *e.g.* [25] for complementary details). The MDKF dynamical system thus reads:

$$\begin{cases} \theta_{k+1} &= \theta_k + w_{\theta,k} \\ 0 &= \nabla_\theta \mathcal{J}(\theta_k,\, Y_k) + v_k \end{cases} \tag{11}$$

This new framework thus differs from classical KFs as measurements are indirectly compared with model predictions through the mCRE functional. Parameter estimates are then sought as minimizers of the mCRE (according to current measurements). The doubt put on the mCRE gradient (with the classical observation noise v) then quantifies the authorized proximity of estimates to the optimal set of parameters that minimizes the mCRE at each time step.

3.2. Technical details about MDKF - Calibration guidelines

The coupling between mCRE and dual Kalman filtering avoids the calibration of process and measurement covariance matrices for state estimation as the state predictions are directly built and processed within the mCRE framework. However, some influential (and tunable) parameters still need to be defined, either following engineering judgement or using automated procedures. These parameters are gathered in Tab. 2. Besides, the MDKF raises several issues regarding:

- the time-frequency domains nested interaction when mixing sequential data assimilation (in time) and mCRE (written in the frequency domain) properly;
- the robustness of the methodology and the calibration of internal parameters. General guidelines must be given on how to adapt the enhanced tools from [10] to a data assimilation framework (namely how to tune r and $z(\omega)$) and how to choose process and measurement noise covariance matrices (Q_θ, R);

- numerical performance and real-time prospects.

These aspects will be discussed in the remainder of this section. An overview of the complete MDKF algorithm is also given (see ALG. 2).

Data assimilation	mCRE functional
• Parameter covariance error matrix Q_θ	• Confidence into measurements coefficient r
• Observer covariance error matrix R	• Frequency weighting function z
• Data assimilation time steps $\{t_k\}$	• Frequency bandwidth D_ω and its sampling

TABLE 2: Listing of the influential parameters related to the MDKF algorithm.

3.2.1. Sliding window technique

The fact that the mCRE operates in the frequency domain implies that a dedicated effort must be made to define how measurements are assimilated by the mCRE functional. Indeed, compared to classical KF approaches, updating parameters for all new data points does not seem relevant as the observer operates on data in the frequency domain. A sliding window technique, whose principle is illustrated in FIG. 2, is thus proposed for handling the time-frequency nested interaction.

The key idea of the sliding window technique proposed here is to process the most recent data block that (partially) includes new assimilated data in order to characterize changes in the measurements frequency content. The design of the sliding window is crucial as it determines the tracking capabilities of MDKF and how fast the changes in structural parameters can be captured. This is especially decisive in cases where abrupt stiffness degrations due to damage may occur.

The design of the sliding window must be done in accordance with the measurements acquisition sampling frequency f_s and the mCRE frequency bandwidth D_ω discretized with a frequency step Δf. The latter must be carefully chosen to correctly capture the frequency content associated to the sollicitated eigenmodes. A common engineering judgement one can recommend is to choose Δf such that the narrowest resonant peak is described by a least three points; considering the 3dB cut-off frequency a simple rule of thumb for the choice of Δf is $3\Delta f \approx \min_i(\xi_i f_i)$, with (ξ_i, f_i) the damping ratio and eigenfrequency of mode i. In the upcoming earthquake-engineering applications, with typical 5% damping ratio values and 2-5 Hz first eigenfrequency values, Δf is chosen within $[0.1\text{ Hz}; 0.5\text{ Hz}]$. Therefore, in order to process accurate Fourier transforms in the mCRE framework, the number of data points N in the projection window must verify:

$$N \geqslant \frac{f_s}{\Delta f} \tag{12}$$

In order to react efficiently to abrupt changes, one should avoid to average the information provided by the newly assimilated data with former measurements. N is thus chosen as the smallest integer satisfying the above inequation. Note that zeropadding can permit to reduce N without decreasing much the FFT accuracy, but it should not be used abusively. Besides, the shape of the window must be carefully chosen due to FFT apodization issues. In the following, Blackman windows are used, as illustrated in FIG. 2.

Algorithm 2: Modified Dual Kalman Filter.

Initialization:

- Sliding window, data assimilation time steps $\{t_k\}$
- mCRE tuning parameters: $D_\omega, r, z(\omega)$ and reduced basis
- Initial statistics on parameters: mean $\widehat{\theta}_0$ and covariance P_0^θ
- Noise process and measurements covariance matrices: Q_θ, R
- Sigma-points weights $\{\mathcal{W}_i^m, \mathcal{W}_i^c\}_{i=0}^{2L}$ with $L = \dim(\widehat{\theta}_0)$

for $k = 0 : \infty$ **do**

1) **Unscented Transform**

Augmented state to include noise parameters:
$\widehat{\theta}_k^a = \left[\widehat{\theta}_k^T \; w_{\theta,k}^T \; v_k^T\right]^T$; $P_k^{\theta,a} = \text{diag}(P_k^\theta, Q_\theta, R)$;
Computation of sigma-points:
$$\mathcal{X}_k^a = \left[\widehat{\theta}_k^a \quad \dots \; \widehat{\theta}_k^a + \sqrt{L+\lambda}\left[P_k^{\theta,a}\right]_j^{1/2} \quad \dots \quad \dots \; \widehat{\theta}_k^a - \sqrt{L+\lambda}\left[P_k^{\theta,a}\right]_j^{1/2} \quad \dots\right]$$

2) **Prediction step**

Direct propagation of the sigma-points through the state update equation:
$\mathcal{X}_{k+1|k}^{i,\theta} = \mathcal{X}_k^{i,\theta} + \mathcal{X}_k^{i,w} \; \forall i \in [\![0; 2L]\!]$;

Computation of *a priori* mean and covariance:
$$\widehat{\theta}_{k+1|k} = \sum_{i=0}^{2L} \mathcal{W}_i^m \mathcal{X}_{k+1|k}^{i,\theta} \; ; P_{k+1|k}^\theta = \sum_{i=0}^{2L} \mathcal{W}_i^c \left(\mathcal{X}_{k+1|k}^{i,\theta} - \widehat{\theta}_{k+1|k}\right)\left(\mathcal{X}_{k+1|k}^{i,\theta} - \widehat{\theta}_{k+1|k}\right)^T ;$$

3) **Processing new data in the frequency domain**

Extraction of the new data block with the sliding window: $y_k(t)$
Fast Fourier transform for mCRE analysis: $Y_k(\omega) \; \forall \omega \in D_\omega$
Possible option: update the frequency weighting function $z(\omega)$

4) **Correction step**

Propagation of the sigma-points through the mCRE functional:
$\mathcal{Y}_{k+1|k}^i = \nabla_\theta \mathcal{J}(\mathcal{X}_{k+1|k}^{i,\theta}, Y_k) + \mathcal{X}_k^{i,v} \; \forall i \in [\![0; 2L]\!]$;

$$\widehat{y}_{k+1|k} = \sum_{i=0}^{2L} \mathcal{W}_i^m \mathcal{Y}_{k+1|k}^i \; ; \; P_{k+1|k}^{yy} = \sum_{i=0}^{2L} \mathcal{W}_i^c \left(\mathcal{Y}_{k+1|k}^i - \widehat{y}_{k+1|k}\right)\left(\mathcal{Y}_{k+1|k}^i - \widehat{y}_{k+1|k}\right)^T ;$$

$$P_{k+1|k}^{\theta y} = \sum_{i=0}^{2L} \mathcal{W}_i^c \left(\mathcal{X}_{k+1|k}^{i,\theta} - \widehat{\theta}_{k+1|k}\right)\left(\mathcal{Y}_{k+1|k}^i - \widehat{y}_{k+1|k}\right)^T ;$$

Correct predictions to compute *a posteriori* statistics:

$K_k = P_{k+1|k}^{\theta y}(P_{k+1|k}^{yy})^{-1}$;
$\widehat{\theta}_{k+1} = \widehat{\theta}_{k+1|k} - K_k \widehat{y}_{k+1|k}$;
$P_{k+1}^\theta = P_{k+1|k}^\theta - K_k P_{k+1|k}^{yy} K_k^T$;

end

Result: Successive estimates of the parameter vector statistics $(\widehat{\theta}_k, P_k^\theta)$

To track at best sudden structural changes, overlapping between windows can also be authorized as long as the Markov process assumption from the KF remains valid. The overlapping rate between two consecutive windows α defines the amount of new assimilated data at each time step. Using α-overlapped windows thus implies that the last $(1-\alpha)N$ data points are new.

Finally, please note that the sliding window also fully conditions the real-time prospects of the MDKF algorithm to the extent that one considers data is assimilated in real-time if the necessary CPU time per iteration is lower than the time between two consecutive data assimilation time steps. Therefore, a compromise has to be found with the overlapping rate α to allow MDKF to perform in real-time and to react fast enough to damage occurrences. A dedicated study in Section 4.1.4 shows the paramount effect of the overlapping rate for accurate real-time identification and confirms that α must be chosen as high as possible and is limited by real-time computational constraints.

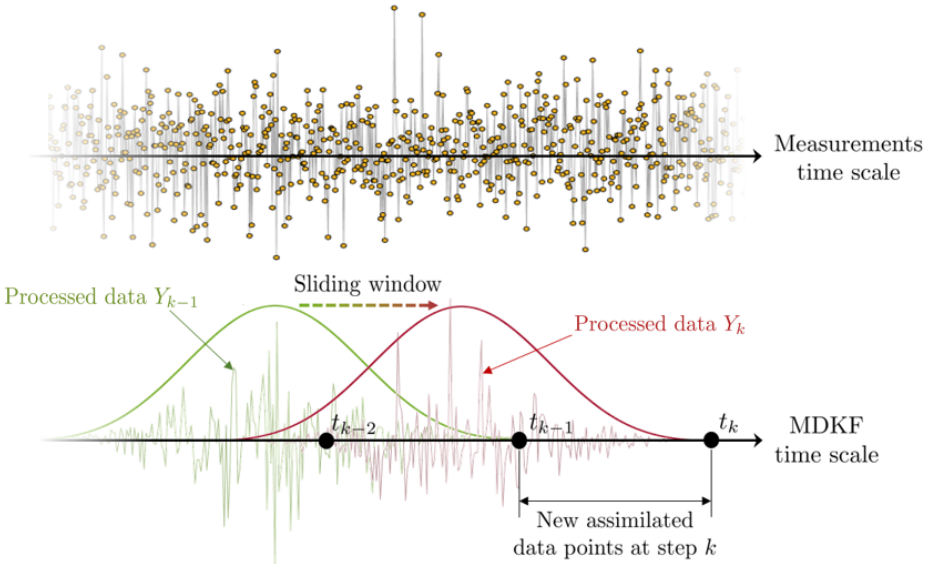


FIGURE 2: Illustration of the sliding window technique for progressive assimilation of data to be processed in the frequency domain by mCRE. A coarse MDKF time scale is defined according to the overlapping rate and the window slides from time step t_{k-1} to t_k to assimilate new available data and identify frequency content changes.

3.2.2. Calibration of MDKF tuning parameters

Contrary to offline model updating algorithms, the mCRE tuning parameters $(r, z(\omega))$ cannot be computed using all the available data since the latter is progressively assimilated. However, after a first training stage, it can be realistically assumed that r and $z(\omega)$ have been already computed from a low-level non-damaging random input using the automated procedures given in [10] before performing data assimilation. Nevertheless, if the value of r is not supposed to be modified during experiments (as it is essentially driven by the measurements SNR), the initial frequency weighting function can become irrelevant if the modal signature of the damaging specimen evolves. In case of important damage occurence, one can possibly update $z(\omega)$ if a strong change in the frequency content is observed, as

noticed in Alg. 2.

The selection of filtering parameters, *i.e.* noise covariance matrices, can affect the performance of the data assimilation process and may even result in a divergence of the algorithm if not well calibrated. Here, some guidelines are given for choosing matrices Q_θ and R (assumed time-invariant). Dividing the state update equation of (11) by the data assimilation time step Δt, one can directly relate the value of Q_θ with the expected possible variation of parameters with time:

$$Q_\theta = \mathbb{E}\left[w_{\theta,k} w_{\theta,k}^T\right] \approx \Delta t^2 \, \mathbb{E}\left[\left(\frac{\partial \theta}{\partial t}\right)\left(\frac{\partial \theta}{\partial t}\right)^T\right] \tag{13}$$

Therefore, assuming the data assimilation time step $\Delta t = (1-\alpha)N/f_s$ to be given by the sliding window technique presented previously, an engineering judgement regarding the possible variability of parameters allows to give a relevant estimation of Q_θ. Regarding the calibration of R, as mentioned above, the observation noise v_k quantifies the tolerance one can have on the expected stationarity of the mCRE gradient. In other words, it tempers the fact that the mCRE may not be exactly minimized by θ_k considering the current measurements Y_k. Even if $R = 0$ is the idealistic case, a small non-zero value of R is used to improve filter convergence as it limits the spurious influence of time steps where data does not store much relevant information for model updating purposes. Typical convenient values of R are given in the following applications.

3.2.3. Computational considerations and real-time prospects

The analysis of Alg. 2 emphasizes the most time-consuming steps of the algorithm (colored in gray), namely the frequency domain data preprocessing and the computation of the mCRE for each set of sigma-points and frequency of D_ω. Even if the call to Fast Fourier Transforms is unavoidable, the computation of the mCRE value for all sigma-points per iteration can be drastically shortened using

(i) reduced basis in order to reduce the size of the system (10) from $2n_x$ to $2n_r$, n_x being the number of dofs and n_r the number of modes stored in the reduced basis. A sufficient number of modes must be considered to cover the frequency range of interest, which is included within the interval [0 Hz; 50 Hz] for most earthquake engineering problems. Therefore, $n_r \gtrsim 20$ is a reasonable choice for the particular case study analyzed here;

(ii) parallelization techniques: the parallel implementation proposed in [45] can be reinvested to overcome the computational burden of UKF (whose CPU time increases significantly with the dimension of the parameter vector to update), and the computation of $\{e_\omega^2\}_{\omega \in D_\omega}$ for the mCRE evaluation can also be distributed.

Doing so, the data processing and correction steps of Alg. 2 can be performed efficiently from a numerical viewpoint, allowing for real-time prospects whatever the initial size of the FE model to update. Finally, please note that data is considered assimilated in real-time if the required CPU time per assimilation time step is lower than the time between two consecutive data assimilation time steps. The real-time limitation is thus not related to the sampling acquisition frequency, but to the MDKF time scale defined by the overlapping rate between consecutive sliding windows (Fig. 2).

4. Numerical applications

In this section, numerical results are presented and discussed to assess MDKF performance for on-the-fly model updating applications. The stiffness parameters of an academic plane frame model are first corrected based on low-SNR measurements obtained from random ground motion input. This application enables to validate the whole procedure and the robustness of the methodology with respect to known measurement noise level by comparison with a classical UKF approach. Afterwards, the SMART2013 shaking-table test campaign database is processed for correcting the associated FE model borrowed from [9]. The quality of the proposed corrections will be assessed by comparing the observed eigenfrequency drop with former data-driven subspace-based experimental identification results [8] and previous mCRE-based model updating results [10]. In both applications, the updated stiffness FE matrix is decomposed in n_θ non-overlapping subdomains and parametrized as follows:

$$K(\theta) = \sum_{i=1}^{n_\theta} \frac{\theta_i}{\theta_{0,i}} K_{0,i} \quad \text{with} \quad K(\theta_0) = \sum_{i=1}^{n_\theta} K_{0,i} \tag{14}$$

The list of reference MDKF tuning parameters used to obtain the forthcoming results is stored in Tab. 3. These values are implicitly used in the following if not specified.

MDKF framework	**Reference value**		
Data sampling frequency	f_s	=	1000 Hz
Overlapping rate for Blackman windows	α	=	90%
mCRE frequency interval	D_ω	=	[1 Hz; 20 Hz]
mCRE frequency sampling step	Δf	=	0.1 Hz
Amount of new data per window	$(1-\alpha)/\Delta f$	=	0.1 s
Covariance on parameter state	Q_θ	=	$10^{-4} I$
Covariance on mCRE	R	=	10^{-8}
Initial covariance on parameters	P_0^θ	=	$0.05 I$

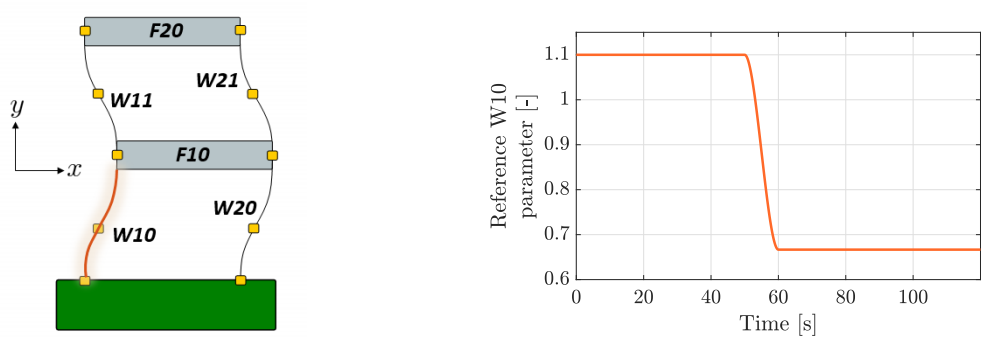
Table 3: Reference setting parameters of the MDKF for the considered applications. I denotes the identity matrix of appropriate dimension.

4.1. Application #1: Academic plane frame submitted to random ground acceleration loading

4.1.1. Description of the problem

We first intend to validate MDKF for parameter estimation from sparse measurements with a typical earthquake engineering academic example. Let us consider the plane frame structure shown in Fig. 3, whose stiffness distribution is assumed unknown. This structure is clamped to a rigid moving support (*e.g.* a shaking-table) and submitted to a 120 s random low-PGA ($0.1g$) bi-axial ground motion input. The reference stiffness field presents a defect that progressively appears in the wall W10 while the initial guess does not perfectly correspond to the healthy reference configuration (10% underestimation). The FE model is made of elastic beam elements and built with the CEA FE simulation software Cast3M©. An intuitive wall/slab decomposition of the frame is chosen: 6 subdomains are defined {W10, W11, W20, W21, F10, F20} (see Fig. 3). The stiffness model to update

on-the-fly is then made of $n_\theta = 6$ parameters. The objective of this academic example is to assess the MDKF ability to recover the expected parameters from simulated acceleration measurements acquired by discrete sensors scattered over the structure (yellow dots in FIG. 3), with particular attention paid to the capability of identifying evolutive parameters.



(a) Subdomains labelling and sensors location.

(b) W10 reference stiffness parameter evolution.

FIGURE 3: Two-story plane frame with sensors location (yellow dots) and subdomains. The progressive damage of wall W10 is marked in orange.

In order to assess the robustness of the methodology with respect to measurement noise, a white noise of known standard deviation is added to the synthetic measurements. The noise level δ (in %) is then defined according to the magnitude of the input ground acceleration $\ddot{U}_d$ such that noisy synthetic acceleration data is obtained as follows:

$$\ddot{y}_{noisy}(t) = \ddot{y}(t) + \delta \ \text{std}\left(\ddot{U}_d(t)\right) \eta(t) \tag{15}$$

where $\eta(t)$ is a random Gaussian vector of zero mean and unitary standard deviation.

4.1.2. MDKF reference data assimilation results

The MDKF algorithm is first assessed using (idealistic) non-noisy acceleration measurements (*i.e.*, $\delta = 0$). Stiffness parameters are correctly updated, as shown in FIG. 4 where the Gaussian probability density functions (pdfs) $\pi(\widehat{\theta}_k|y_{0:k})$ of the (assumed unknown) parameters are successively plotted at each data assimilation time step. The close correlation of the pdfs with the reference parameter values as well as the tightness of confidence intervals illustrate the relevance of MDKF for on-the-fly model updating. Besides, even though the first time step is longer as not enough data has been assimilated to perform accurate FFTs (10 s-long sliding window), the short time response in the first iterations emphasizes that all parameters are quickly and correctly identified. Moreover, the decay of the W10 parameter is well monitored by the algorithm, with an unevitable slight delay due to the use of the sliding window. This is certainly the main drawback of the proposed approach. Note also that the update of the time-evolutive W10 parameter does not lead the algorithm to erroneous local minima. Finally, one can notice that lower-story parameters (associated to subdomains W10, W20, F10 having higher energetic participation) are estimated with more confidence by the MDKF. Indeed, the comparison of pdfs width shows that more doubt remains in the identified values of subdomains W11, W21 and F20 as they are less sensitive

to the model updating problem. However, the estimated means remain close to the reference values, which highlights how MDKF can explicitly provide relevant information regarding (relative) uncertainties of estimates.

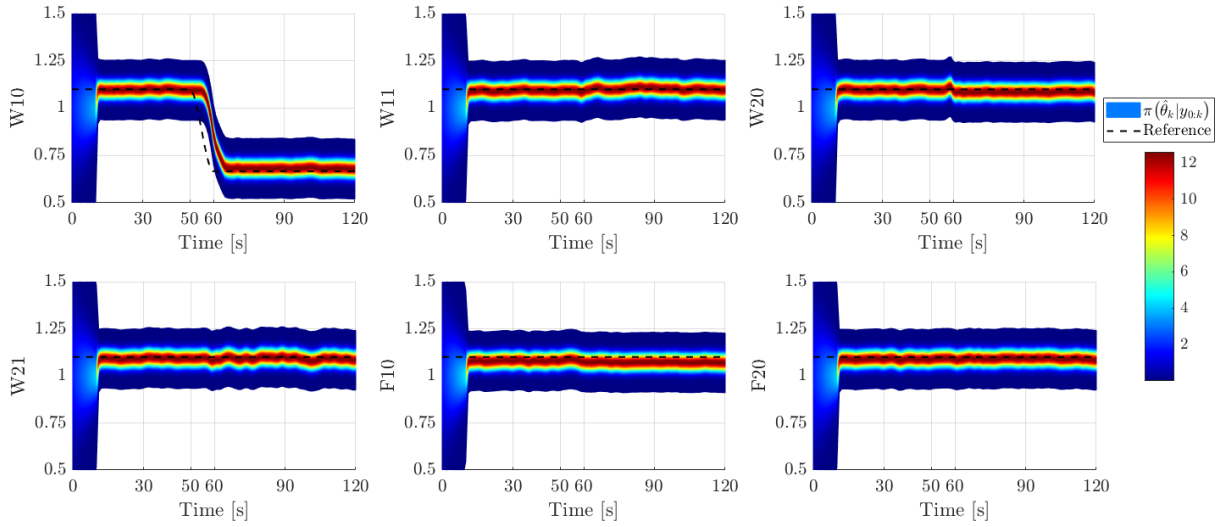


FIGURE 4: MDKF data assimilation results of the frame FE model from non-noisy measurements ($\delta = 0\%, r = 0.1$). Probability density functions are plotted for each stiffness parameter with expected values to identify.

4.1.3. MDKF enhanced robustness with respect to measurement noise

For real-life realistic applications, the stability and robustness of the MDKF with respect to measurement noise must be addressed. In FIG. 5, low-SNR measurements (with $\delta = 20\%$) are successfully assimilated. As measurement noise disturbs the data assimilation process, the credible interval identified for all parameters becomes larger. Besides, the mean estimates $\widehat{\theta}_k$ are also oscillating around the expected value due to the fact that noise directly impacts the convexity of the mCRE functional. The difference in terms of sensitivity between subdomains (W10, W20, F10) and (W11, W21, F20) is even more significant.

Due to the fact that the MDKF benefits from mCRE properties, the data assimilation algorithm shows a different behaviour compared to classical nonlinear KFs with respect to measurement noise. Indeed, as mCRE tuning parameters are automatically adapted to measurement SNR, the MDKF algorithm directly takes into account the reliability of available data through the mCRE observer. In particular, the estimated means of parameters tend to (slowly) oscillate around the target values rather than being systematically biased (no offset) and increasing the noise level does not affect the reactivity of MDKF to quickly correct the initial model guess bias (observed by comparison of FIG. 4 and 5).

4.1.4. Impact of the sliding window design

As mentioned in Section 3.2.1, the design of the sliding window must be made with caution so as to guarantee a compromise between real-time computational constraints and reactivity to detect defects accurately. In FIG. 6, we show the necessity to correctly calibrate

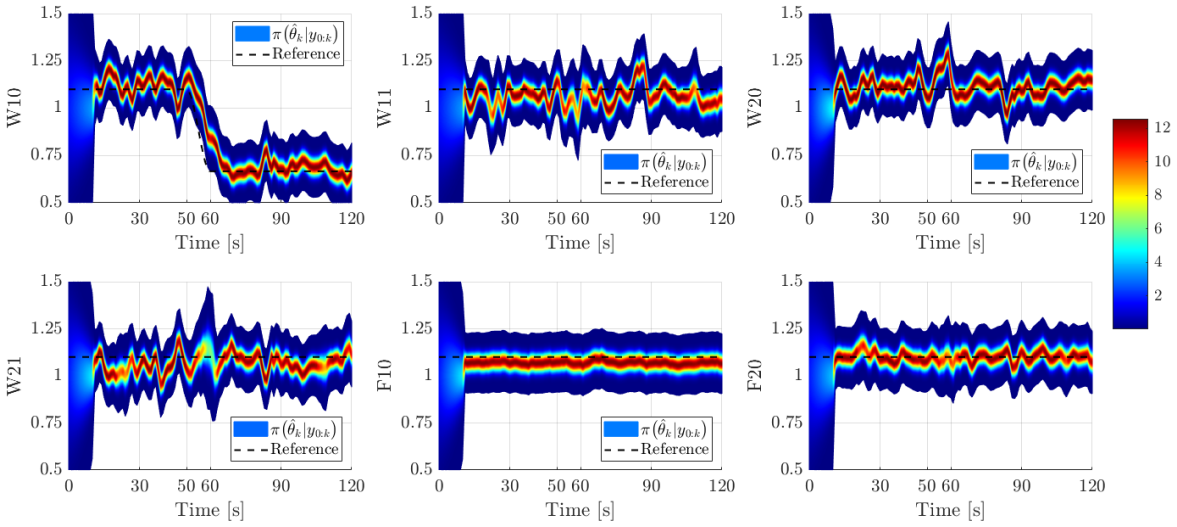


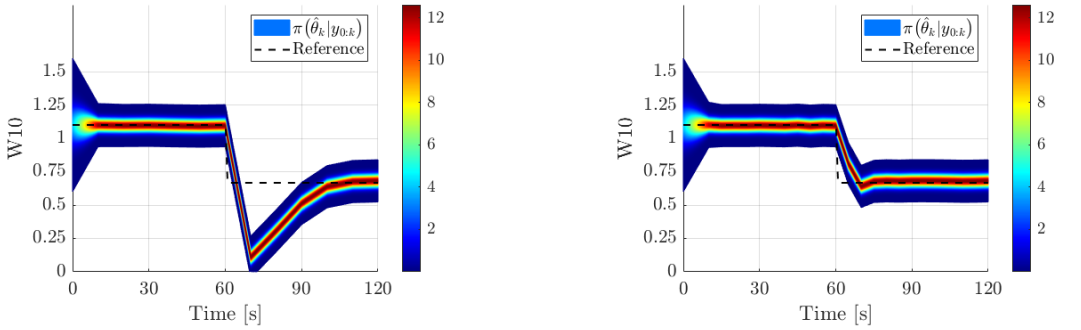
FIGURE 5: MDKF data assimilation results of the frame FE model from noisy measurements ($\delta = 20\%, r = 0.01$). Probability density functions are plotted for each stiffness parameter with expected values to identify.

the overlapping rate between consecutive windows α when trying to track a local sudden stiffness change appearing in W10 subdomain. Low values let a lot of remaining CPU time available between iterations (to perform post-processing operations) but are not reactive enough to follow sudden stiffness changes whereas high values do not enable MDKF to perform in real-time. The $\alpha = 90\%$ value defined in 3 appears to be a good compromise between accurate parameter tracking and real-time CPU constraints.

Finally, one can again observe the slight delay due to the use of the sliding window, which is unevitable and due to the time-frequency domains nested interaction through the mCRE functional: in order to guarantee accurate frequency content to be processed by the mCRE, the number of time points N cannot be restrained to the new assimilated measurement alone. Although this is probably the main limit of the method, we expect it not to impact much the additional post-processing operations. The computational burden of the latter could also be of valuable help to calibrate α at best.

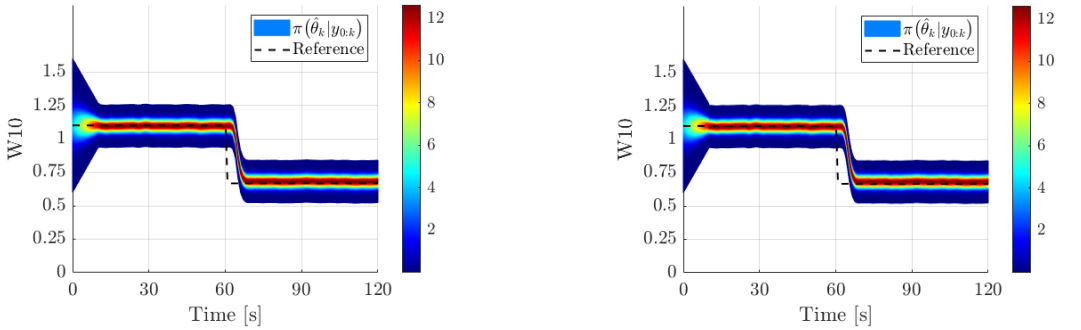
4.1.5. Comparison between MDKF and standard UKF

One could even legitimately question the interest of MDKF in comparison with the classical data assimilation methods mentioned in Section 1 and 2. Although it is well known that nonlinear KFs can loss accuracy with high noise levels [49], a dedicated comparison in the current case study with joint UKF (implemented according to ALG. 1) has been performed. Key results are shown in FIG. 7 for the tracking of the W10 (evolutive) stiffness parameter. One can first observe that the mean value identified using the classical joint UKF (JUKF) is much more oscillating than the one provided by the MDKF. Besides, JUKF estimates hardly correspond to the expected value after $t = 60$ s, showing here the limitations of classical approaches to recover damage parameters from acceleration measurements using explicit time integration schemes as model operator. As a consequence, the width of credible intervals



(a) $\alpha = 0\%$
Remaining time between data assimilation steps: 9.83 s

(b) $\alpha = 50\%$
Remaining time between data assimilation steps: 4.83 s



(c) $\alpha = 90\%$
Remaining time between data assimilation steps: 0.83 s

(d) $\alpha = 99\%$
Data assimilation steps are too long of 0.08 s

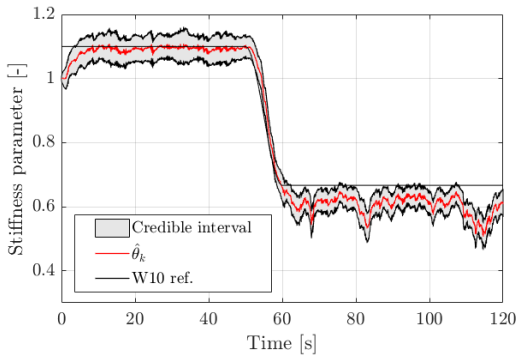
FIGURE 6: Impact of the overlapping rate between consecutive sliding windows to track sudden stiffness changes accurately.

shows the lack of confidence in the estimates provided by JUKF. On the contrary, MDKF parameter estimates are much more stable in time, whatever the noise level δ. Another important remark relates to the calibration of the JUKF tuning parameters, which is a complex task without any *a priori* idea about the intrinsic relevance of both model and measurements. In particular, the compromise between Q_x, Q_θ and R is a sensitive user-made manipulation that strongly conditions the quality of JUKF estimates. Finally, whether for joint or dual UKF, the amount of sigma-points to be propagated at each data assimilation time step is a major limitation considering real-time applications prospects (justifying that recent works involve reduced order modeling techniques). As a reminder, note that these two limitations are circumvented by the MDKF algorithm.

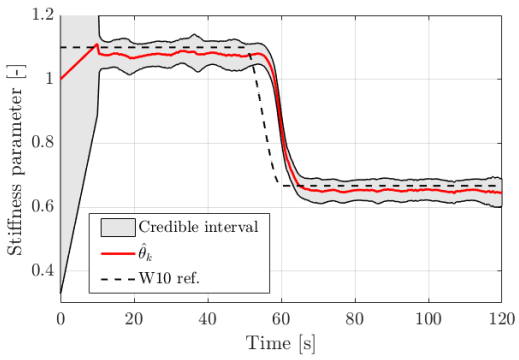
4.1.6. Calibration of MDKF tuning parameters and real-time prospects

As the calibration of classical KFs covariance error matrices strongly impacts parameter estimates, a complete study regarding the influence of internal parameters of MDKF that may affect its performance must be done. As the reference parameters $\theta^\star(t)$ are known in this academic example, an overall performance indicator, denoted ϵ, can be defined:

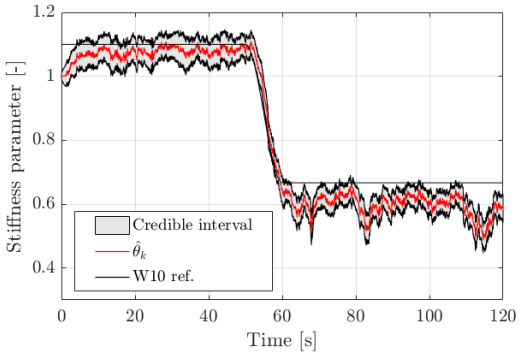
$$\epsilon = \frac{\|\theta^\star(t) - \widehat{\theta}(t)\|_{L_2}^2}{\|\theta^\star(t)\|_{L_2}^2} \quad \text{with} \quad \|\square\|_{L_2}^2 \triangleq \int_0^T \square^2 \, \mathrm{d}t \tag{16}$$



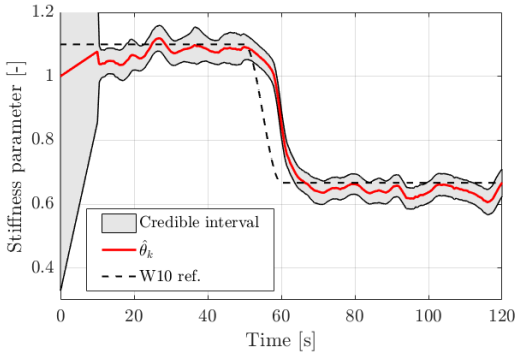
(a) JUKF - $\delta = 0\%, Q_x = 10^{-8}I, Q_\theta = 10^{-7}I, R = 10^{-2}I$



(b) MDKF - $\delta = 0\%, r = 0.5$



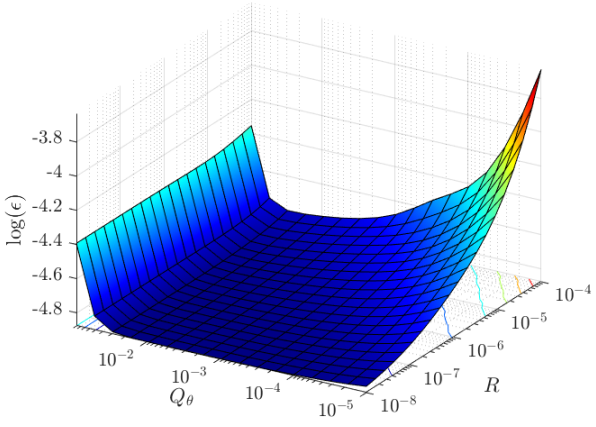
(c) JUKF - $\delta = 20\%, Q_x = 10^{-8}I, Q_\theta = 10^{-7}I, R = 10^{-2}I$



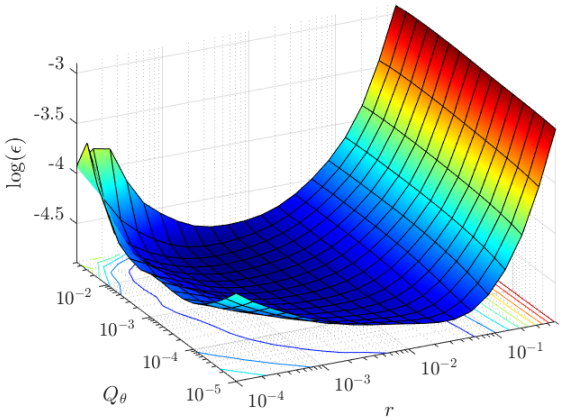
(d) MDKF - $\delta = 20\%, r = 0.001$

FIGURE 7: Comparison of JUKF and MDKF for the identification of the W10 stiffness parameter from acceleration measurements. Credible intervals are defined at $\pm 3\sigma_\theta$.

where T is the duration of the test. The computation of this performance indicator allows to carry out a sensitivity analysis on the key parameters of the MDKF algorithm, namely Q_θ, R and r, whose results are presented in FIG. 8.



(a) $\log(\epsilon)$ as function of Q_θ and R



(b) $\log(\epsilon)$ as function of Q_θ and r

FIGURE 8: Impact of tuning parameters Q_θ, R and r on the performance of MDKF from noisy measurements ($\delta = 10\%$).

Even if this analysis is computationally expensive and not possible in realistic applications (only because reference parameters are not always known), several remarks can be made:

(i) there exists a set of optimal parameters that minimize the error between the estimated mean and reference parameters (for a given dataset);

(ii) sub-optimal choices for Q_θ, R, r (*i.e.* values close to the optimum) are yet leading to correct and acceptable results. Indeed, there is no need to select the optimum value among Q_θ, R, r to get satisfying results. For instance, observing FIG. 8.a, Q_θ can be merely adjusted between 10^{-4} and 10^{-2} and MDKF will still provide accurate results. Actually for this example, any couple (Q_θ, R, r) that verifies $\log \epsilon < -4.5$ is convenient. These results suggest that the general guidelines provided in Section 3.2.2 are sufficient to calibrate tuning parameters correctly;

(iii) the optimal values provided by the plots of FIG. 8 do not take into account the width of credible intervals, which is of major importance if the complete parameter statistics are post-processed.

Finally, note that the overlapping rate α is also of major importance as it defines how data is progressively assimilated. As mentioned above, its value fully conditions the real-time prospects of MDKF as data is considered assimilated in real-time if the required CPU time per iteration is lower than the time between two consecutive data assimilation time steps. Numerical tests have shown that $\alpha > 80\%$ was a convenient compromise between accuracy and computational time. Indeed, the projection of (10) using small-size truncated modal basis and the parallelization of numerical operations of sigma-points allow a large computational speed-up whatever the size of the considered FE model. Doing so, the results presented above have been obtained processing measurements faster than they were assimilated. With an overlapping rate $\alpha = 90\%$, 1 s-overlapped windows were assimilated in less than 0.2 s using a personal laptop (Dell Latitude 7310 - 8Go RAM - Intel i5 1.70 GHz processor). The computational burden carried by the numerous calls to mCRE is thus considerably reduced. Considering realistic applications, the remaining available CPU time could be exploited to update mCRE tuning parameters (in particular $z(\omega)$) or to communicate with the experimental system in order to adapt control laws in a DDDAS context (see FIG. 1).

4.2. Application #2: On-the-fly correction of the SMART2013 RC model from acceleration time histories

4.2.1. Presentation of the benchmark

In order to assess the vulnerability of reinforced concrete (RC) structures subjected to torsional effects during seismic ground motions, the SMART2013 experimental test campaign was conducted in the CEA/TAMARIS facility at the end of 2013. A three-story 1/4 reduced-scale trapezoidal RC specimen clamped on the six dofs AZALEE shaking-table has been subjected to a sequence of gradually damaging seismic tests (FIG. 9). Equipped with eight 1000kN maximum capacity hydraulic MTS actuators, the AZALEE shaking-table can reproduce complex seismic motions (six independent movements: three rotations and three

translations) on large scale specimens. The test sequence consisted in an alternation of bi-axial gradually damaging seismic inputs of increasing level and of random ground motions with low acceleration level chosen such that the first eigenmodes of the experimental system are excited but without adding further damage to the RC specimen. A brief recap of the SMART2013 test campaign is given in Tab. 4.

The specimen was instrumented with more than 200 sensors including 64 capacitive accelerometers of ±10 g range scattered over the RC specimen. 48 out of these latter (pointed on Fig. 9 by orange circles) have been used as experimental reference for correcting the FE model, whose mesh is also displayed in Fig. 9. More precisely, accelerations were recorded at the corners of the trapezoid on each story (including soleplate level), while vertical accelerations were measured in-between the masses at floor levels. Measurements were acquired at a sample frequency of 1000 Hz and filtered with 400 Hz cut-off frequency anti-aliasing filters. A typical ±0.003 g white noise level was observed on the accelerometers. The displacements and accelerations of the eight hydraulic rods of the Azalee shaking-table were also measured, providing complete and redundant access to the input imposed on the specimen.

The reference FE model has been developed in the Cast3M© FE framework using multi-layered shell and Timoshenko multi-fiber beam elements (see Fig. 9); it is fully described in [9]. The call to a model updating procedure makes sense when observing the strong gaps between the predicted and the experimental eigenfrequencies (see Tab. 5). This FE model has already been used in [10] for model updating purposes, making thus a relevant reference point for assessing how the MDKF can process actual measurements on-the-fly. For additional details about the SMART2013 benchmark, the interested reader is referred to [8, 9].

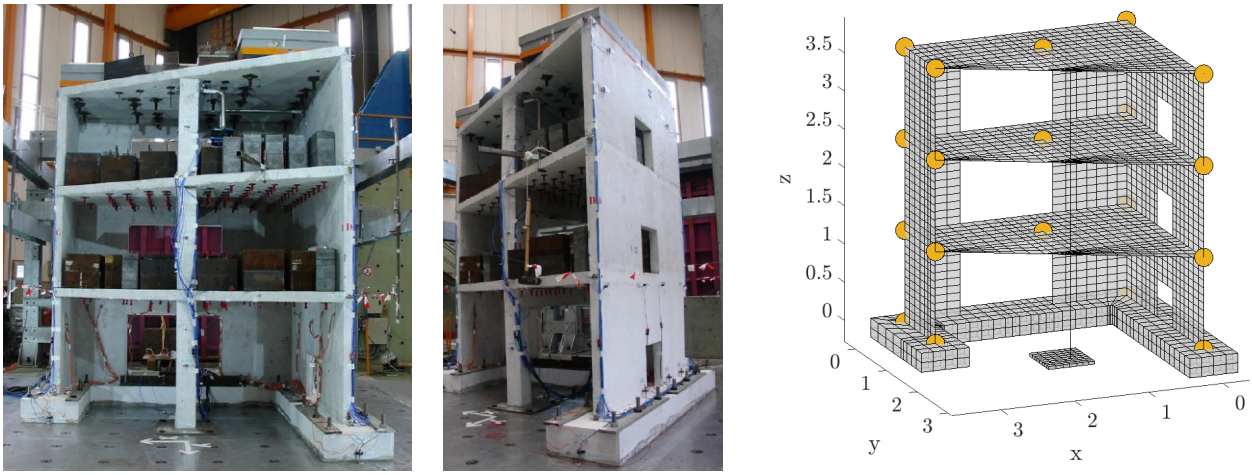


Figure 9: The SMART2013 specimen anchored to the Azalee shaking-table and the associated FE model, where orange circles indicate the location of accelerometers used for the on-the-fly model updating strategy.

4.2.2. Applicability of MDKF to the online correction of the SMART2013 model

The non-damaging low-PGA tests allow to iteratively adapt the linear control laws according to the observed eigenfrequency drop. However, when the specimen response becomes

Phase 1: SMART2008 inputs - PGA$(x, y) = (0.2g, 0.2g)$		δ [%]
Run #6	Broad-band bi-axial signal $(x+y)$ $0.02g$ RMS	22.6
Run #7	Seismic signal - 50%	-
Run #8	Broad-band bi-axial signal $(x+y)$ $0.02g$ RMS	29.0
Run #9	Seismic signal - 100%	-
Phase 2: Northridge main shock signal - PGA$(x, y) = (1.78g, 0.99g)$		
Run #10	Broad-band bi-axial signal $(x+y)$ $0.02g$ RMS	23.8
Run #11	Seismic signal - 11%	-
Run #12	Broad-band bi-axial signal $(x+y)$ $0.02g$ RMS	31.1
Run #13	Seismic signal - 22%	-
Run #14	Broad-band bi-axial signal $(x+y)$ $0.02g$ RMS	26.1
Run #15	Seismic signal - 22%	-
Run #16	Broad-band bi-axial signal $(x+y)$ $0.02g$ RMS	28.5
Run #17	Seismic signal - 44%	-
Run #18	Broad-band bi-axial signal $(x+y)$ $0.02g$ RMS	28.0
Run #19	Seismic signal - 100%	-
Phase 3: Northridge after-shock signal - PGA$(x, y) = (0.37g, 0.31g)$		
Run #20	Broad-band bi-axial signal $(x+y)$ $0.02g$ RMS	20.1
Run #21	Seismic signal 33%	-
Run #22	Broad-band bi-axial signal $(x+y)$ $0.02g$ RMS	26.0
Run #23	Seismic signal 100%	-
Run #24	Broad-band bi-axial signal $(x+y)$ $0.02g$ RMS	22.5

TABLE 4: Synthesis of the SMART2013 shaking-table tests and SNR δ for the low-PGA random tests.

Mode number	Experimental eigenfrequencies [Hz]	Initial model	
		Frequency [Hz]	Error [%]
1	6.28	9.10	44.8
2	9.22	15.72	70.5
3	17.6	31.77	80.5

TABLE 5: SMART2013 - Comparison of the first eigenfrequencies and relative errors between the experimental reference [8] and the initial FE model.

strongly nonlinear (due to damage) within a seismic test, the control strategy fails to keep the input stable: it has been the case for Run #13 where the end of the run became unstable after important damage occured at the bottom of the specimen (see FIG. 10). To avoid such issues, the control strategy must integrate a tool allowing for online monitoring of eigenfrequencies.

One should first notice that classical KFs fail at properly tracking eigenfrequencies: we applied a classical UKF algorithm with the above-described FE model projected on a truncated modal basis made of the first 100 eigenmodes of the cantilevered specimen (in order to be competitive enough in terms of CPU time). Unfortunately, despite all attempts to calibrate covariance matrices properly, the algorithm systematically diverged (negative stiffness parameter estimates). This can be explained by the fact that the model to update is too stiff to properly describe the observed state of the structure (see Table 5). Contrary to

classical KFs, mechanical fields are not explicitly integrated in the MDKF as only the mCRE gradient value is exploited in the correction step of the algorithm. This allows MDKF to still be relevant in cases where classical KFs fail at identifying parameters due to strong model discrepancies.

In order to assess the relevance of the proposed methodology in this context, the MDKF algorithm is carried out on the complete SMART2013 database and post-processing CPU-time inspection shall allow us to conclude on the suitability of the approach for further online applications. Practically:

- a precalibration test (based on run #6 data) allows to estimate relevant values for mCRE tuning parameters $r = 0.01$ and $z(\omega)$. As for the previous case, covariance error matrices are set to $Q_\theta = 10^{-4} I, R = 10^{-8}$.
- the measurements of all runs are gathered into a single data block, meaning the campaign from Run #6 to #24 is processed at once. The frequency weighting function is updated after each low-PGA-input block as new ergodic data is available for computing $z(\omega)$ as explained in [10].
- once parameter statistics $\{\widehat{\theta}_k, P_k^\theta\}$ are provided, a low-cost post-processing step consists in propagating parameters uncertainties to relevant quantities of interest, namely the first (sollicitated) eigenfrequencies. The suitability of MDKF for adaptive control law design can then be judged from eigenfrequencies mean values and associated credible intervals. Of course, the question of the definition of the FE model parametrization is a problem of its own that also directly impacts the performance of the algorithm. This point will not be addressed in the remainder of this section for the sake of conciseness, but a full discussion with application to the SMART2013 case is available in [10].

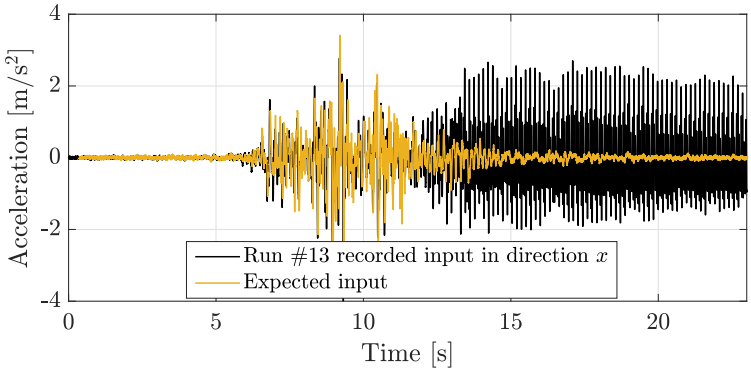


FIGURE 10: SMART2013 Run #13 - shaking-table input measurement becoming unstable due to damage occurence at the bottom of the specimen.

Data assimilation results obtained after processing the complete SMART2013 database are given in FIG. 11 - 12 - 13. Several remarks can be made regarding:

- **MDKF suitability for DDDAS and adaptive control law design**

Using the dedicated strategies for enhanced numerical performance explained in Section 3.2.3 allows to process data faster than they are assimilated as 0.5 s-overlapped data windows are assimilated in less than 0.3 s on a personal laptop (Dell Latitude 7310 - 8Go RAM - Intel i5 1.70 GHz processor). Here again, the computational burden carried by the numerous calls to mCRE is thus considerably reduced, the most time-consuming operation being the frequency domain data preprocessing step.

Beyond the possibility to track the evolution of eigenfrequencies in real-time, the MDKF is particularly able to process strongly nonlinear runs, where *a posteriori* model updating methods are unable to provide any result without data preprocessing (see the focus on the run #13 in Fig. 13). The information provided by MDKF could then be valuable for avoiding unstable testings in a complete DDDAS framework. This will be the topic of forthcoming research work.

Finally, let us remark that the call for reduced basis when computing the mCRE permits an important computational speed-up, whatever the initial complexity of the FE model to update. This feature suggests that MDKF (and mCRE in general) could be applied to a wide range of online model updating problems.

- **The applicability of MDKF to online structural monitoring**

The proposed data assimilation algorithm is able to update the general stiffness parameter of a linear FE model in order to track the structural state of a specimen subjected to complex nonlinear phenomena. The new MDKF algorithm has been able to assimilate data in real-time (regarding CPU-time, according to the above definition) and provided parameter estimates that allow (after post-processing) to observe the eigenfrequency drop that was reported after the experimental campaign [9]. In particular, two stages in the test campaign where the modal signature remains globally constant have been well recovered: runs #6 to #12 (phase 1: SMART2008 inputs), and #20 to #24 (phase 3: after-shock analysis).

Besides, the similarities between MDKF estimates and (i) former results from stochastic subspace identification [8] and (ii) former mCRE-based model updating [10] confirm the relevance of parameter estimates provided by MDKF (see Fig. 11-12).

Unfortunately for the SMART2013 case, even if a large number of sensors are scattered over the specimen (48 data acquisitions channels), the experimental information they bring is not rich enough to locally quantify the damage state of the specimen, which is a critical issue for SHM perspectives. Although the processed database can be considered rich, the initial gap between the updated model and the highly-noisy ($\eta > 20\%$) data collected from the experimental campaign do not allow us to perform realistic SHM in this application. However, please note that even when performing offline mCRE-based and least-square-based model updating from the SMART2013 database, we have not been able to identify more than one global stiffness parameter in [10]. Therefore, we must point out that the SMART2013 database itself seems hardly exploitable for damage detection problems and SHM, which cannot allow us to draw proper conclusions about the applicability of MDKF for SHM in this specific context.

- **The intrinsic quality of the updated model**

Here, contrary to the plane frame problem where $n_\theta = 6$ parameters were updated at once, the FE model has only been parametrized with one global stiffness parameter. Indeed, although this simplistic parametrization choice is enough for control prospects, it is certain that the corrections of the FE stiffness matrix proposed herein may lack of relevance for local damage detection purposes. Let us recall that the noise level always exceeds 20% (see TAB. 4), which makes the identification of stiffness parameters tough. The same issue has been raised in [10] when performing offline model updating from the SMART2013 database using mCRE and total least-square functionals.

If measurements were less noisy and sensors more focalized on the bottom of the specimen (which has been shown to be the more sensitive area for stiffness parameters of cantilevered structures in [10]), we are convinced that more parameters would have been identified, whether in offline or online model updating contexts. This issue is a current subject of extensive research: we are investigating the limitations and capabilities of mCRE and MDKF for SHM, in particular regarding the sensor placement strategy and the information that can be extracted from several types of measurements (displacement, acceleration, strain, optic fiber measurements). Regarding the SMART2013 FE model itself, the anchorage boundary conditions that fully cantilever the specimen to the shaking-table should be questioned. Indeed, an overestimation of the anchorage stiffness (due to the combination of integrated shell elements and volumic elements at the soleplate level) may lead to a globally too rigid FE model.

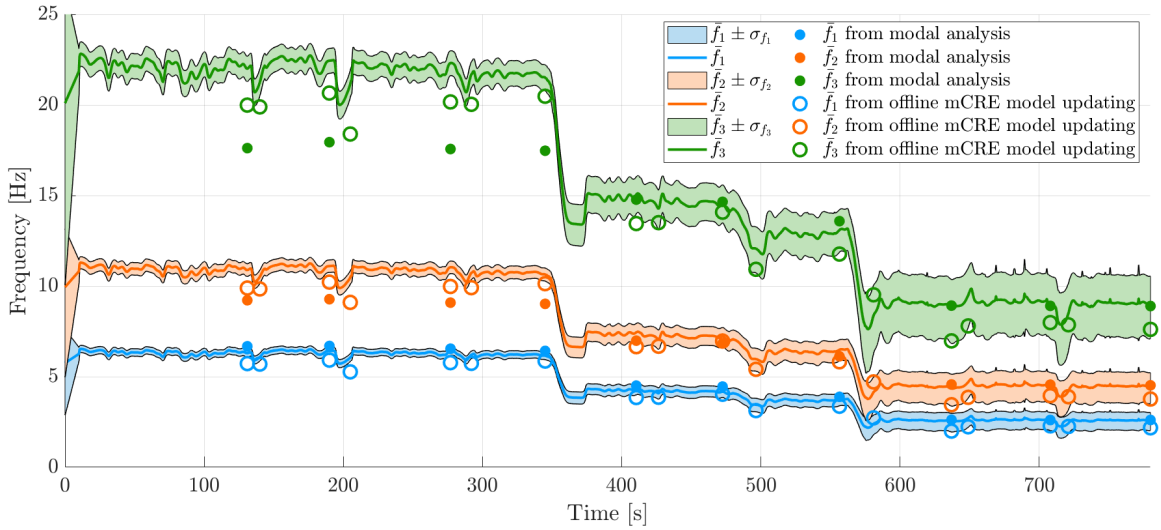


FIGURE 11: SMART2013 - Tracking of the three first eigenfrequencies using MDKF. Mean and credible intervals are given, as well as former identification results using SSI techniques ([8] in colored bullets) and offline mCRE-based model updating ([10] in colored circles) for comparison purposes.

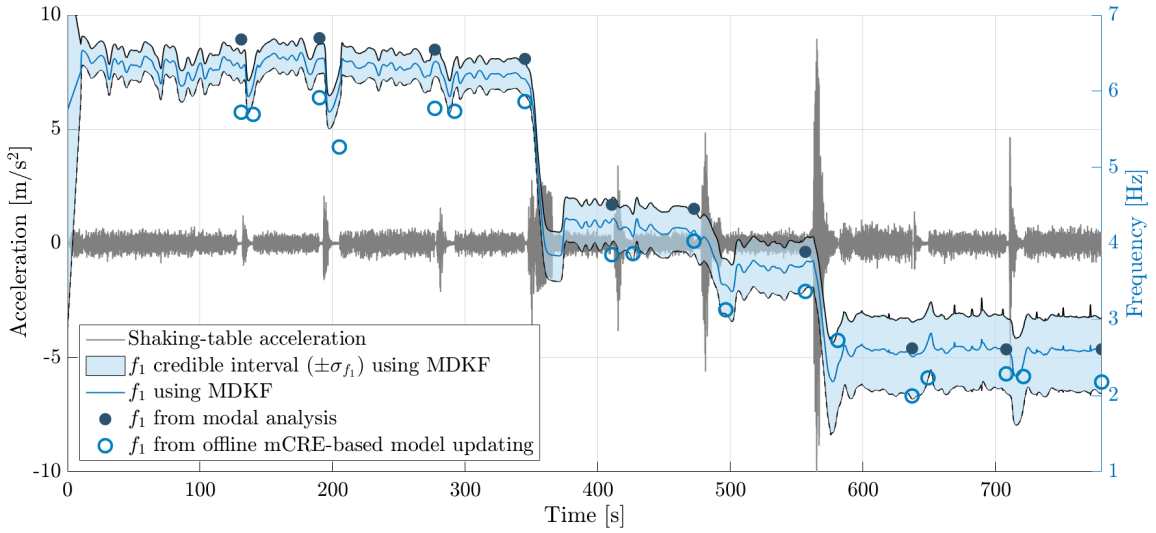


FIGURE 12: SMART2013 - Focus on the first eigenfrequency using MDKF. The shaking-table acceleration recordings in the x-direction are given to relate inputs with structural state evolution.

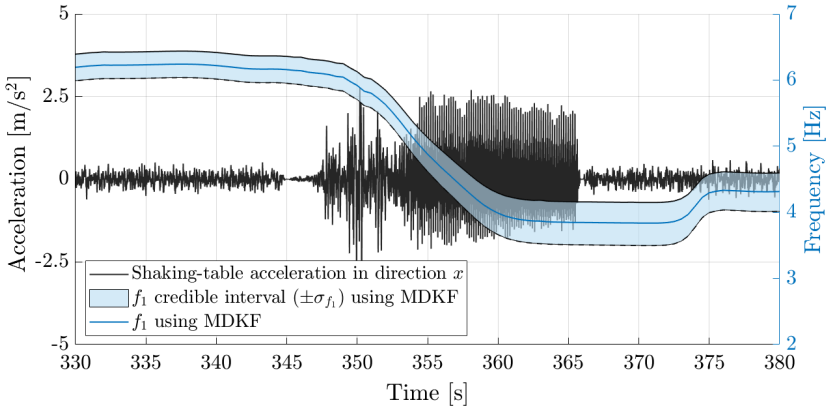


FIGURE 13: SMART2013 - Focus on Run #13. Although the control strategy becomes unstable, MDKF still identifies damage occurence and updates eigenfrequencies adequately.

5. Conclusions and prospects

In this paper, a sequential data assimilation method for monitoring the state of structures in low-frequency dynamics was proposed. A strategy for correcting on-the-fly FE stiffnesses by exploiting at best a set of available measurements was discussed. This new approach derives a Dual Kalman Filter framework in which the measurement update metric has been changed using the modified Constitutive Relation Error functional (mCRE). This new online model updating algorithm, called Modified Dual Kalman Filter (MDKF), combines KF and mCRE advantages as it proposes a sequential data assimilation with enhanced robustness with respect to measurement noise.

Although intuitively constraining at the first sight because of the mCRE definition in the frequency domain, the MDKF has shown relevant performance from synthetic and actual measurements, both in terms of accuracy and CPU time. Indeed, the comparison with

classical UKF on an academic plane frame example illustrated the relevance of the MDKF which is able to perform accurate and robust identification of stiffness properties in real-time, whatever the complexity of the FE model under study. Then, the complete processing of the SMART2013 experimental database highlighted (i) the ability of the MDKF for on-the-fly eigenfrequency tracking and (ii) the robustness of the algorithm to update a linear FE model from sparse data involving many nonlinear phenomena. General guidelines were also provided regarding the calibration of MDKF internal tuning parameters in order to avoid conditioning the performance of the method to an expert-user's judgment. Even though a full automation of the MDKF algorithm is not obtained yet (and is currently investigated), the positive results obtained herein show the potential of this new sequential data assimilation algorithm.

Consequently, the proposed MDKF seems to be a relevant tool to perform online stiffness monitoring of structures submitted to low-frequency dynamics loading conditions. It could also be involved in a DDDAS framework, such as the one that motivated this study since the mCRE-based tools for system identification are promising for quantifying stiffness loss (if data is informative enough). Compared to the discrete eigenfrequency values obtained with offline modal analysis, the estimates provided on-the-fly by MDKF are valuable assets for control prospects. The next step will aim at closing the feedback loop to perform model-based control (Fig. 1) by using at best the information provided by MDKF to improve shaking-table experiments for vulnerability assessment of civil engineering structures subjected to seismic hazard. As mentioned above in the analysis of SMART2013 identification results, the applicability of the MDKF to SHM must be addressed, particularly the question of damage detection from sparse data. Current studies are conducted in that sense to properly bound the capabilities of mCRE for damage detection in SHM applications. The mCRE-oriented optimal sensor placement problem also naturally raises. Finally, an issue not addressed in this contribution deals with the optimal choice of the parameter space, which seems crucial for an optimal identification, *i.e.* at low-cost both in terms of CPU time and compatibility with available measurements. Coupling MDKF with adaptive parameter space description may be an appropriate solution as the CRE, which is a local model quality indicator, is directly available from the mCRE computation requirements. It may lead to a sequential data assimilation scheme where model parametrization is refined only if needed, allowing for optimal identification at minimal cost.

Acknowledgements

The authors would like to thank the CEA and EDF for providing the material support required to carry out this work. The work reported in this paper has also been supported by the SEISM Institute (http://www.institut-seism.fr). C. Gauchy and C. Feau are particularly thanked for their deep interest and numerous advices that were of great help to shape this contribution in its current form.

References

[1] F. Chinesta, E. Cueto, E. Abisset-Chavanne, J. L. Duval, F. E. Khaldi, Virtual, Digital and Hybrid Twins: A New Paradigm in Data-Based Engineering and Engineered Data,

Archives of Computational Methods in Engineering 27 (1) (2018) 105–134. doi:10.1007/s11831-018-9301-4.
URL http://link.springer.com/10.1007/s11831-018-9301-4

[2] A. Rasheed, O. San, T. Kvamsdal, Digital Twin: Values, Challenges and Enablers From a Modeling Perspective, IEEE Access 8 (2020) 21980–22012, conference Name: IEEE Access. doi:10.1109/ACCESS.2020.2970143.

[3] T. Ritto, F. Rochinha, Digital twin, physics-based model, and machine learning applied to damage detection in structures, Mechanical Systems and Signal Processing 155 (2021) 107614. doi:10.1016/j.ymssp.2021.107614.
URL https://linkinghub.elsevier.com/retrieve/pii/S0888327021000091

[4] F. Darema, Dynamic Data Driven Applications Systems: A New Paradigm for Application Simulations and Measurements, in: M. Bubak, G. D. van Albada, P. M. A. Sloot, J. Dongarra (Eds.), Computational Science - ICCS 2004, Lecture Notes in Computer Science, Springer, Berlin, Heidelberg, 2004, pp. 662–669. doi:10.1007/978-3-540-24688-6_86.

[5] L. Chamoin, Merging advanced sensing techniques and simulation tools for future structural health monitoring technologies, The Project Repository Journal 10 (1) (2021) 124–127. doi:10.54050/PRJ10124127.

[6] E. N. Chatzi, M. N. Chatzis, C. Papadimitriou (Eds.), Robust Monitoring, Diagnostic Methods and Tools for Engineered Systems, Frontiers Research Topics, Frontiers Media SA, 2020. doi:10.3389/978-2-88966-088-9.

[7] O. Avci, O. Abdeljaber, S. Kiranyaz, M. Hussein, M. Gabbouj, D. J. Inman, A review of vibration-based damage detection in civil structures: From traditional methods to Machine Learning and Deep Learning applications, Mechanical Systems and Signal Processing 147 (2021) 107077. doi:10.1016/j.ymssp.2020.107077.
URL https://linkinghub.elsevier.com/retrieve/pii/S0888327020304635

[8] P.-E. Charbonnel, Fuzzy-driven strategy for fully automated modal analysis: Application to the SMART2013 shaking-table test campaign, Mechanical Systems and Signal Processing 152 (2021) 107388. doi:10.1016/j.ymssp.2020.107388.
URL https://linkinghub.elsevier.com/retrieve/pii/S0888327020307743

[9] B. Richard, S. Cherubini, F. Voldoire, P.-E. Charbonnel, T. Chaudat, S. Abouri, N. Bonfils, SMART2013: Experimental and numerical assessment of the dynamic behavior by shaking table tests of an asymmetrical reinforced concrete structure subjected to high intensity ground motions, Engineering Structures 109 (2016) 99–116. doi:10.1016/j.engstruct.2015.11.029.

[10] M. Diaz, P.-É. Charbonnel, L. Chamoin, Robust energy-based model updating framework for random processes in dynamics: application to shaking-table experiments, Computers and Structures (2022). doi:https://doi.org/10.1016/j.compstruc.2022.106746.
URL https://hal.archives-ouvertes.fr/hal-03528432

[11] M. Bonnet, A. Constantinescu, Inverse problems in elasticity, Inverse Problems 21 (2) (2005) R1–R50. doi:10.1088/0266-5611/21/2/R01.
URL https://iopscience.iop.org/article/10.1088/0266-5611/21/2/R01

[12] A. Tarantola, Inverse Problem Theory and Methods for Model Parameter Estimation, Society for Industrial and Applied Mathematics, 2005. doi:10.1137/1.9780898717921.
URL http://epubs.siam.org/doi/book/10.1137/1.9780898717921

[13] F. M. Hemez, S. W. Doebling, Review and assessment of model updating for nonlinear, transient dynamics, Mechanical Systems and Signal Processing 15 (1) (2001) 45–74. doi:10.1006/mssp.2000.1351.
URL https://linkinghub.elsevier.com/retrieve/pii/S0888327000913517

[14] A. Teughels, G. De Roeck, Damage detection and parameter identification by finite element model updating, Archives of Computational Methods in Engineering 12 (2) (2005) 123–164. doi:10.1007/BF03044517.
URL https://doi.org/10.1007/BF03044517

[15] J. E. Mottershead, M. Link, M. I. Friswell, The sensitivity method in finite element model updating: A tutorial, Mechanical Systems and Signal Processing 25 (7) (2011) 2275–2296. doi:10.1016/j.ymssp.2010.10.012.
URL https://linkinghub.elsevier.com/retrieve/pii/S0888327010003316

[16] J. Kaipio, E. Sommersalo, Statistical Inversion Theory, in: Statistical and Computational Inverse Problems, 2005, pp. 49–114.

[17] E. Simoen, G. De Roeck, G. Lombaert, Dealing with uncertainty in model updating for damage assessment: A review, Mechanical Systems and Signal Processing 56-57 (2015) 123–149. doi:10.1016/j.ymssp.2014.11.001.
URL https://linkinghub.elsevier.com/retrieve/pii/S0888327014004130

[18] N. Maia, M. Reynier, P. Ladevèze, Error Localization for Updating Finite Element Models Using Frequency-response-functions, in: SPIE - INTERNATIONAL SOCIETY FOR OPTICAL ENGINEERING, 1994.

[19] A. T. Chouaki, P. Ladevèze, L. Proslier, Updating Structural Dynamic Models with Emphasis on the Damping Properties, AIAA Journal 36 (6) (1998) 1094–1099, publisher: American Institute of Aeronautics and Astronautics _eprint: https://doi.org/10.2514/2.486. doi:10.2514/2.486.
URL https://doi.org/10.2514/2.486

[20] P. Ladevèze, A. Chouaki, Application of a posteriori error estimation for structural model updating, Inverse Problems 15 (1) (1999) 49–58, publisher: IOP Publishing. doi:10.1088/0266-5611/15/1/009.
URL https://doi.org/10.1088/0266-5611/15/1/009

[21] A. Deraemaeker, P. Ladevèze, P. Leconte, Reduced bases for model updating in structural dynamics based on constitutive relation error, Computer Methods in Applied Mechanics and Engineering 191 (21-22) (2002) 2427–2444. doi:10.1016/S0045-7825(01)00421-2.
URL https://linkinghub.elsevier.com/retrieve/pii/S0045782501004212

[22] A. Deraemaeker, P. Ladevèze, T. Romeuf, Model validation in the presence of uncertain experimental data, Engineering Computations 21 (8) (2004) 808–833. doi:10.1108/02644400410554335.

URL https://www.emerald.com/insight/content/doi/10.1108/02644400410554335/full/html

[23] P. Ladevèze, D. Leguillon, Error estimate procedure in the finite element method and applications, SIAM Journal on Numerical Analysis 20 (3) (1983) 485–509. doi:https://doi.org/10.1137/0720033.

[24] W. Aquino, M. Bonnet, Analysis of the error in constitutive equation approach for time-harmonic elasticity imaging, SIAM Journal on Applied Mathematics 79 (3) (2019) 822–849, arXiv:1812.03653.
URL http://arxiv.org/abs/1812.03653

[25] P.-E. Charbonnel, P. Ladevèze, F. Louf, C. Le Noac'h, A robust CRE-based approach for model updating using in situ measurements, Computers & Structures 129 (2013) 63–73. doi:10.1016/j.compstruc.2013.08.002.
URL https://linkinghub.elsevier.com/retrieve/pii/S0045794913002216

[26] P. Feissel, O. Allix, Modified constitutive relation error identification strategy for transient dynamics with corrupted data: The elastic case, Computer Methods in Applied Mechanics and Engineering 196 (13-16) (2007) 1968–1983. doi:10.1016/j.cma.2006.10.005.
URL https://linkinghub.elsevier.com/retrieve/pii/S0045782506003434

[27] M. Ben Azzouna, P. Feissel, P. Villon, Robust identification of elastic properties using the Modified Constitutive Relation Error, Computer Methods in Applied Mechanics and Engineering 295 (2015) 196–218. doi:10.1016/j.cma.2015.04.004.
URL https://linkinghub.elsevier.com/retrieve/pii/S0045782515001486

[28] E. Barbarella, O. Allix, F. Daghia, J. Lamon, T. Jollivet, A new inverse approach for the localization and characterization of defects based on compressive experiments, Computational Mechanics 57 (6) (2016) 1061–1074. doi:10.1007/s00466-016-1278-y.
URL http://link.springer.com/10.1007/s00466-016-1278-y

[29] T. Silva, N. Maia, Detection and localisation of structural damage based on the error in the constitutive relations in dynamics, Applied Mathematical Modelling 46 (2017) 736–749. doi:10.1016/j.apm.2016.07.002.
URL https://linkinghub.elsevier.com/retrieve/pii/S0307904X16303833

[30] B. Banerjee, T. F. Walsh, W. Aquino, M. Bonnet, Large scale parameter estimation problems in frequency-domain elastodynamics using an error in constitutive equation functional, Computer Methods in Applied Mechanics and Engineering 253 (2013) 60–72. doi:10.1016/j.cma.2012.08.023.
URL https://linkinghub.elsevier.com/retrieve/pii/S0045782512002770

[31] S. Guchhait, B. Banerjee, Constitutive error based parameter estimation technique for plate structures using free vibration signatures, Journal of Sound and Vibration 419 (2018) 302–317. doi:10.1016/j.jsv.2018.01.020.
URL https://linkinghub.elsevier.com/retrieve/pii/S0022460X18300282

[32] R. Ferrier, A. Cocchi, C. Hochard, Modified constitutive relation error for field identification: Theoretical and experimental assessments on fiber orientation identification in a composite

material, International Journal for Numerical Methods in Engineering (2021) nme.6842doi:10.1002/nme.6842.
URL https://onlinelibrary.wiley.com/doi/10.1002/nme.6842

[33] R. Bouclier, F. Louf, L. Chamoin, Real-time validation of mechanical models coupling PGD and constitutive relation error, Computational Mechanics 52 (4) (2013) 861–883. doi:10.1007/s00466-013-0850-y.
URL http://link.springer.com/10.1007/s00466-013-0850-y

[34] R. E. Kalman, A New Approach to Linear Filtering and Prediction Problems, Journal of Basic Engineering 82 (1) (1960) 35–45. doi:10.1115/1.3662552.
URL https://doi.org/10.1115/1.3662552

[35] R. E. Kalman, When Is a Linear Control System Optimal?, Journal of Basic Engineering 86 (1) (1964) 51–60. doi:10.1115/1.3653115.
URL https://doi.org/10.1115/1.3653115

[36] M. S. Grewal, A. P. Andrews, Kalman Filtering: Theory and Practice Using MATLAB, 1st Edition, Wiley, 2008. doi:10.1002/9780470377819.
URL https://onlinelibrary.wiley.com/doi/book/10.1002/9780470377819

[37] G. Evensen, The ensemble kalman filter: Theoretical formulation and practical implementation, Ocean Dynamics 53 (2003) 343–367. doi:10.1007/s10236-003-0036-9.

[38] E. N. Chatzi, A. W. Smyth, The unscented kalman filter and particle filter methods for nonlinear structural system identification with non-collocated heterogeneous sensing, Structural Control and Health Monitoring 16 (1) (2009) 99–123. arXiv:https://onlinelibrary.wiley.com/doi/pdf/10.1002/stc.290, doi:https://doi.org/10.1002/stc.290.
URL https://onlinelibrary.wiley.com/doi/abs/10.1002/stc.290

[39] S. Julier, J. Uhlmann, H. Durrant-Whyte, A new method for the nonlinear transformation of means and covariances in filters and estimators, IEEE Transactions on Automatic Control 45 (3) (2000) 477–482. doi:10.1109/9.847726.
URL http://ieeexplore.ieee.org/document/847726/

[40] S. Julier, The scaled unscented transformation, in: Proceedings of the 2002 American Control Conference (IEEE Cat. No.CH37301), IEEE, Anchorage, AK, USA, 2002, pp. 4555–4559 vol.6. doi:10.1109/ACC.2002.1025369.
URL http://ieeexplore.ieee.org/document/1025369/

[41] E. Wan, R. Van Der Merwe, The unscented Kalman filter for nonlinear estimation, in: Proceedings of the IEEE 2000 Adaptive Systems for Signal Processing, Communications, and Control Symposium (Cat. No.00EX373), IEEE, 2000, pp. 153–158. doi:10.1109/ASSPCC.2000.882463.
URL http://ieeexplore.ieee.org/document/882463/

[42] R. Van Der Merwe, Sigma-Point Kalman Filters for Probabilistic Inference in Dynamic State-Space Models, Ph.D. thesis, Oregon Health & Science University (2004).

[43] M. Hoshiya, E. Saito, Structural Identification by Extended Kalman Filter, Journal of Engineering Mechanics 110 (12) (1984) 1757–1770. doi:10.1061/(ASCE)0733-9399(1984)110:12(1757).
URL http://ascelibrary.org/doi/10.1061/%28ASCE%290733-9399%281984%29110%3A12%281757%29

[44] S. Eftekhar Azam, M. Bagherinia, S. Mariani, Stochastic system identification via particle and sigma-point Kalman filtering, Scientia Iranica 19 (4) (2012) 982–991. doi:10.1016/j.scient.2012.06.007.
URL https://linkinghub.elsevier.com/retrieve/pii/S1026309812001289

[45] S. Eftekhar Azam, A. Ghisi, S. Mariani, Parallelized sigma-point Kalman filtering for structural dynamics, Computers & Structures 92-93 (2012) 193–205. doi:10.1016/j.compstruc.2011.11.004.
URL https://linkinghub.elsevier.com/retrieve/pii/S0045794911002811

[46] S. Eftekhar Azam, Online Damage Detection in Structural Systems, SpringerBriefs in Applied Sciences and Technology, Springer International Publishing, Cham, 2014. doi:10.1007/978-3-319-02559-9.
URL http://link.springer.com/10.1007/978-3-319-02559-9

[47] S. Eftekhar Azam, E. Chatzi, C. Papadimitriou, A dual Kalman filter approach for state estimation via output-only acceleration measurements, Mechanical Systems and Signal Processing 60-61 (2015) 866–886. doi:10.1016/j.ymssp.2015.02.001.
URL https://linkinghub.elsevier.com/retrieve/pii/S0888327015000746

[48] S. Eftekhar Azam, S. Mariani, Online damage detection in structural systems via dynamic inverse analysis: A recursive Bayesian approach, Engineering Structures 159 (2018) 28–45. doi:10.1016/j.engstruct.2017.12.031.
URL https://linkinghub.elsevier.com/retrieve/pii/S0141029617320813

[49] S. Mariani, A. Ghisi, Unscented Kalman filtering for nonlinear structural dynamics, Nonlinear Dynamics 49 (1-2) (2007) 131–150. doi:10.1007/s11071-006-9118-9.
URL http://link.springer.com/10.1007/s11071-006-9118-9

[50] M. Wu, A. W. Smyth, Application of the unscented Kalman filter for real-time nonlinear structural system identification, Structural Control and Health Monitoring 14 (7) (2007) 971–990. doi:10.1002/stc.186.
URL https://onlinelibrary.wiley.com/doi/10.1002/stc.186

[51] P. Moireau, D. Chapelle, Reduced-order Unscented Kalman Filtering with application to parameter identification in large-dimensional systems, ESAIM: Control, Optimisation and Calculus of Variations 17 (2) (2011) 380–405. doi:10.1051/cocv/2010006.
URL http://www.esaim-cocv.org/10.1051/cocv/2010006

[52] A. Onat, A Novel and Computationally Efficient Joint Unscented Kalman Filtering Scheme for Parameter Estimation of a Class of Nonlinear Systems, IEEE Access 7 (2019) 31634–31655. doi:10.1109/ACCESS.2019.2902368.
URL https://ieeexplore.ieee.org/document/8656464/

[53] R. Astroza, H. Ebrahimian, J. P. Conte, Performance comparison of Kalman-based filters for nonlinear structural finite element model updating, Journal of Sound and Vibration 438 (2019) 520–542. doi:10.1016/j.jsv.2018.09.023.
URL https://linkinghub.elsevier.com/retrieve/pii/S0022460X18306084

[54] R. Astroza, A. Alessandri, J. P. Conte, A dual adaptive filtering approach for nonlinear finite element model updating accounting for modeling uncertainty, Mechanical Systems and Signal Processing 115 (2019) 782–800. doi:10.1016/j.ymssp.2018.06.014.
URL https://linkinghub.elsevier.com/retrieve/pii/S0888327018303510

[55] M. Song, R. Astroza, H. Ebrahimian, B. Moaveni, C. Papadimitriou, Adaptive Kalman filters for nonlinear finite element model updating, Mechanical Systems and Signal Processing 143 (2020) 106837. doi:10.1016/j.ymssp.2020.106837.
URL https://linkinghub.elsevier.com/retrieve/pii/S0888327020302235

[56] T. Lefebvre, H. Bruyninckx, J. De Schutter, Kalman filters for non-linear systems: a comparison of performance, International Journal of Control 77 (7) (2004) 639–653. doi:10.1080/00207170410001704998.
URL http://www.tandfonline.com/doi/abs/10.1080/00207170410001704998

[57] S. Mariani, A. Corigliano, Impact induced composite delamination: state and parameter identification via joint and dual extended Kalman filters, Computer Methods in Applied Mechanics and Engineering 194 (50-52) (2005) 5242–5272. doi:10.1016/j.cma.2005.01.007.
URL https://linkinghub.elsevier.com/retrieve/pii/S0045782505000320

[58] A. Hommels, A. Murakami, S.-I. Nishimura, A comparison of the ensemble kalman filter with the unscented kalman filter: application to the construction of a road embankment, in: 19th European Young Geotechnical Engineers' Conference, Vol. 13, Citeseer, 2008.

[59] M. Cheng, T. C. Becker, Performance of unscented kalman filter for model updating with experimental data, Earthquake Engineering and Structural Dynamics 50 (2021) 1948–1966. doi:10.1002/eqe.3426.

[60] B. Marchand, L. Chamoin, C. Rey, Real-time updating of structural mechanics models using Kalman filtering, modified constitutive relation error, and proper generalized decomposition: Real-time updating of structural mechanics models, International Journal for Numerical Methods in Engineering 107 (9) (2016) 786–810. doi:10.1002/nme.5197.
URL https://onlinelibrary.wiley.com/doi/10.1002/nme.5197

[61] W. Li, S. Sun, Y. Jia, J. Du, Robust unscented Kalman filter with adaptation of process and measurement noise covariances, Digital Signal Processing 48 (2016) 93–103. doi:10.1016/j.dsp.2015.09.004.
URL https://www.sciencedirect.com/science/article/pii/S1051200415002729